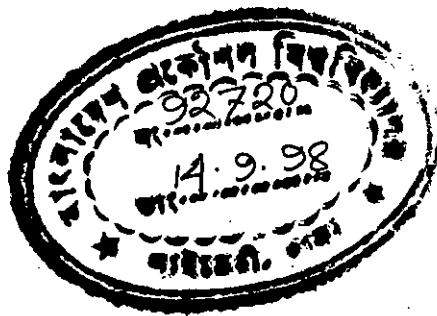


IMPACT OF SELF- PHASE MODULATION ON OPTICAL CPFSK SYSTEM

A Thesis submitted to the Electrical and Electronic Engineering Department of
BUET, Dhaka, in partial fulfillment of the requirements for the degree of
Master of Science in Engineering
(Electrical & Electronic)



623.80414
1998
SAR

BIKASH CHANDRA SARKER



June 1998

DEDICATED TO
THE DEPARTED SOUL OF MY SISTER

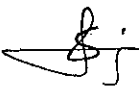
APPROVAL

The thesis titled “**Impact of Self-phase Modulation on Optical CPFSK System**” submitted by Bikash Chandra Sarker, Roll no-921311F, Session 1990-91-92 to the Electrical and Electronic Engineering Department of BUET has been accepted as satisfactory for partial fulfillment of the requirements for the degree of Master of Science in Engineering (Electrical and Electronic)

Board of Examiners

1. Dr. Satya Prasad Majumder
Professor
Department of EEE
BUET, Dhaka-1000.

Chairman
(Supervisor)


19.7.98

2. Dr. Enamul Basher
Professor and Head
Department of EEE
BUET, Dhaka-1000.

Member
(Ex-officio)

E. Basher
19.7.98

3. Dr. Saifur Rahman
Professor,
Department of EEE
BUET, Dhaka-1000.

Member



4. Md. Ashraful Alim
Director, Planning
Bangladesh T & T Board
37/E, Eskaton Garden, Dhaka-1000.

Member
(External)



DECLARATION

This work has been done by me and it has not been submitted elsewhere for the award of any degree or diploma.

Countersigned

 19.7.98
(Dr. Satya Prasad Majumder)

 19.7.98
(Bikash Chandra Sarker)

Supervisor

ACKNOWLEDGEMENTS

The author would like to express his sincere and profound gratitude to his supervisor Dr. Satya Prasad Majumder, Professor, Department of Electrical and Electronics Engineering, BUET for his meticulous guidance, friendly supervision and constant encouragement in completing the work. The also thanks him specially for his valuable suggestions and help during the vital phases of the work.

The author wishes to express his thanks and regards to Dr. Enamul Baser, Professor and Head of the Department of Electrical and Electronics Engineering, BUET for his support and encouragement to complete this work successfully.

The author would like to thank Dr. Saifur Rahman, Professor of EEE, BUET, Dr. Pran Kanai Shaha, Associate Professor of EEE, BUET and many other faculty members of this Department for their cooperation, suggestions and encouragement.

Lastly, the author likes to thank his friends and colleagues especially Tipu Sarker, Ritu sarker, Md. Nasiruddin, Md. Rafiqul Islam, Md. Hasanuzzaman for their support, continuous inspiration and constant encouragement to complete this work and also remembers his departed beloved sister for her blessings.

CONTENTS

Approval	iii
Declaration	iv
Acknowledgments	v
Contents	vi
Abstract	viii
List of Figures	ix
List of Principal Symbols	xv
List of Abbreviations	xvii
Chapter 1 : Introduction	1
1.1 Introduction to Optical Communication	1
1.2 Limitations of Optical Fibre Communications	6
1.3 Brief Review of Previous Works	7
1.4 Objectives of the Study	10

Chapter 2 : Effect of GVD and SPM on Optical CPFSK System	11
2.1 Overview	11
2.2 System Model	13
2.2.1 Direct Detection CPFSK	13
2.2.2 Operation of MZI	16
2.2.3 MZI Characteristics	16
2.3 Theoretical analysis for DD-CPFSK	18
2.4 Theoretical Analysis of Heterodyne CPFSK	29
Chapter 3 : Results and Discussions	34
Chapter 4 : Conclusion and Suggestions for Future Works	64
4.1 Conclusion	64
4.2 Suggestions for Future Works	66
References	67

ABSTRACT

A detail theoretical analysis is presented for direct detection optical CPFSK and heterodyne optical CPFSK system with Mach-zehnder Interferometer (MZI) as an optical frequency discriminator (OFD). The analysis is carried out taking into account the combined effect of Self-phase Modulation and chromatic dispersion of optical fibre. Fluctuation in signal power due to GVD causes a random phase modulation of the signal itself due to nonlinear refractive index of fibre. The effect is termed as self-phase-modulation (SPM) and causes spectral broadening of the transmitted signal and higher bandwidth requirement and degrades receiver performance. The statistics of the signal phase fluctuations at the output of the fibre caused by non-linear filtering due to chromatic dispersion are to be determined in terms of its moments and the probability density function (pdf) of the random phase fluctuation due to SPM and fibre chromatic dispersion. The analysis also includes the effect of GVD and laser phase noise. The method is based on the linear approximation of the output phase of a linearly filtered angle-modulated signal such as the CPFSK signal considered in this work. An equivalent transfer function of a single mode fibre is derived which includes the effects of SPM in presence of GVD. The overall degradation in signal phase is also derived following by an analytical approach. The expression for BER is then derived considering the effects of GVD and SPM in presence of laser phase noise and receiver noise. The analysis is carried out for both direct detection receiver and heterodyne delay demodulation receiver.

Using the noise statistics and moments, the bit error rate (BER) performance of the receiver is then evaluated for different values of input power at different modulation index at a bit rate of 10 Gbit/s. The penalty suffered by the system due to dispersion and Self-phase modulation is then determined at a BER of 10^{-9} . For different fibre length penalty is measured individually for direct detection and heterodyne CPFSK system. Also for negative dispersion coefficient the penalty is determined. Finally, theoretical results are compared with the results obtained from simulation.

LIST OF FIGURES

- Fig.1.1 Generalized block diagram of an optical communication system.
- Fig.2.1 Block diagram of an FSK direct detection receiver with Mach-zehnder Interferometer (MZI) as an optical frequency discriminator (OFD).
- Fig.2.2 (a) An MZI with large ΔL or narrow wavelength spacing,
(b) Transmittance characteristics of an MZI and
(c) Differential output of the balanced receiver.
- Fig.2.3 Output phase response of single mode fibre for rectangular input phase with fibre span length $L=50$ km, $P_{in} = -5$ dBm.
- Fig.2.4 (a) Output phase response of single mode fibre for rectangular input phase with fibre span length $L=100$ km, $P_{in} = -5$ dBm.
(b) Output phase response of single mode fibre for rectangular input phase with fibre span length $L=100$ km, $P_{in} = 0$ dBm.
(c) Output phase response of single mode fibre for rectangular input phase with fibre span length $L=100$ km, $P_{in} = 10$ dBm.
- Fig.2.5 Variation of Mean square phase error (MSE) with respect to Chromatic dispersion index γ , for CPFSK ($h=1$) and MSK ($h=0.5$) obtained by simulation.
- Fig.2.6 Block diagram of an optical heterodyne CPFSK system.

Fig.3.1 The bit error rate (BER) performance of direct detection optical CPFSK system at a bit rate 10 Gb/s with fibre chromatic dispersion $D_c = 15$ ps/km-nm, band width $B=0.75$, fibre length $L=40$ km, wavelength of 1550 nm and modulation index $h=1.0$ for different values of received power P_s (dBm) at the receiver terminal.

Fig.3.2 The bit error rate (BER) performance of direct detection optical CPFSK system at a bit rate 10 Gb/s with fibre chromatic dispersion $D_c=15$ ps/km-nm, band width $B=0.75$, fibre length $L=40$ km, wavelength of 1550 nm and modulation index $h=0.5$ for different values of received power P_s (dBm) at the receiver terminal.

Fig.3.3 The bit error rate (BER) performance of direct detection optical CPFSK system at a bit rate 10 Gb/s with fibre chromatic dispersion $D_c=15$ ps/km-nm, band width $B=0.75$, fibre length $L=80$ km, wavelength of 1550 nm and modulation index $h=1.0$ for different values of received power P_s (dBm) at the receiver terminal.

Fig.3.4 The bit error rate (BER) performance of direct detection optical CPFSK system at a bit rate 10 Gb/s with fibre chromatic dispersion $D_c=15$ ps/km-nm, band width $B=0.75$, fibre length $L=120$ km, wavelength of 1550 nm and modulation index $h=1.0$ for different values of received power P_s (dBm) at the receiver terminal.

Fig.3.5 The bit error rate (BER) performance of direct detection optical CPFSK system at a bit rate 10 Gb/s with fibre chromatic dispersion $D_c=-15$ ps/km-nm, band width $B=0.75$, fibre length $L=120$ km, wavelength of 1550 nm and modulation index $h=1.0$ for different values of received power P_s (dBm) at the receiver terminal.

- Fig.3.6 Plots of penalty in signal power due to Self-phase-modulation & fibre chromatic dispersion at $BER=10^{-9}$ versus power input with bit rate $Br=10$ Gb/s, dispersion co-efficient $D_c=15$ ps/km-nm, band width $B=0.75$ and modulation index $h=1.0$ for different lengths $L=40$ km, 60 km, 80 km, 120 km at a Direct detection CPFSK receiver.
- Fig.3.7 Plots of penalty in signal power due to Self-phase-modulation & fibre chromatic dispersion at $BER=10^{-9}$ versus power input with bit rate $Br=10$ Gb/s, dispersion coefficient $D_c=15$ ps/km-nm, band width $B=0.75$ and modulation index $h=0.5$ for different lengths $L=40$ km, 60 km, 80 km, 120 km at a Direct detection CPFSK receiver.
- Fig.3.8 Plots of penalty in signal power due to Self-phase-modulation & fibre chromatic dispersion at $BER=10^{-9}$ versus power input with bit rate $Br=10$ Gb/s, dispersion coefficient $D_c=-15$ ps/km-nm, band width $B=0.75$ and modulation index $h=1.0$ for different lengths $L=40$ km, 60 km, 80 km, 120 km at a direct detection CPFSK receiver.
- Fig.3.9 Plots of penalty in signal power due to Self-phase-modulation & fibre chromatic dispersion at $BER=10^{-9}$ versus power input with bit rate $Br=10$ Gb/s, dispersion coefficient $D_c=-15$ ps/km-nm, band width $B=0.75$ and modulation index $h=0.5$ for different lengths $L=40$ km, 60 km, 80 km, 120 km at a direct detection CPFSK receiver.
- Fig3.10 Variation of the bit error rate (BER) performance due to different values of modulation index (say, $h=0.6, 0.8$) of a direct detection CPFSK receiver at a bit rate 10 Gb/s with fibre chromatic dispersion $D_c=15$ ps/km-nm, fibre length $L=40$ km, band width $B=0.75$, for several values of received power P_s .

Fig.3.11 Variation of power penalty in signal power due to combined effect of Self-phase-modulation & fibre chromatic dispersion at $BER=10^{-9}$ versus modulation index (h) with fibre length $L=40\text{km}$, $Br=10\text{ Gb/s}$, dispersion coefficient $D_c=15$ and band width $B_{IF}=2$ for different values of input power $P_{in}=-10, 0, 15\text{ dB}$ for a direct detection CPFSK receiver.

Fig.3.12 Variation of power penalty in signal power due to combined effect of Self-phase-modulation & fibre chromatic dispersion at $BER=10^{-9}$ versus modulation index (h) with fibre length $L=40\text{km}$, $Br=10\text{ Gb/s}$, dispersion coefficient $D_c=15$ and band width $B_{IF}=2$ for different values of input power $P_{in}=15, 7.5, 0.0\text{ dBm}$ for a direct detection CPFSK receiver.

Fig.3.13 The bit error rate (BER) performance of a heterodyne optical CPFSK system at a bit rate 10 Gb/s with fibre chromatic dispersion $D_c=-15\text{ ps/km-nm}$, band width $B_{IF}=2$, fibre length $L=40\text{ km}$, wavelength of 1550 nm and modulation index $h=1.0$ for different values of received power $P_s\text{ (dBm)}$ at the receiver terminal.

Fig.3.14 The bit error rate (BER) performance of a heterodyne optical CPFSK system at a bit rate 10 Gb/s with fibre chromatic dispersion $D_c=-15\text{ ps/km-nm}$, band width $B_{IF}=2$, fibre length $L=40\text{ km}$, wavelength of 1550 nm and modulation index $h=0.5$ for different values of received power $P_s\text{ (dBm)}$ at the receiver terminal.

Fig.3.15 The bit error rate (BER) performance of a heterodyne optical CPFSK system at a bit rate 10 Gb/s with fibre chromatic dispersion $D_c=-15\text{ ps/km-nm}$, band width $B_{IF}=2$, fibre length $L=80\text{ km}$, wavelength of 1550 nm and modulation index $h=1.0$ for different values of received power $P_s\text{ (dBm)}$ at the receiver terminal.

Fig.3.16 The bit error rate (BER) performance of a heterodyne optical CPFSK system at a bit rate 10 Gb/s with fibre chromatic dispersion $D_c=+15$ ps/km-nm, band width $B_{IF}=2$, fibre length $L=80$ km, wavelength of 1550 nm and modulation index $h=1.0$ for different values of received power P_s (dBm) at the receiver terminal.

Fig.3.17 The bit error rate (BER) performance of a heterodyne optical CPFSK system at a bit rate 10 Gb/s with fibre chromatic dispersion $D_c=-15$ ps/km-nm, band width $B_{IF}=2$, fibre length $L=120$ km, wavelength of 1550 nm and modulation index $h=1.0$ for different values of received power P_s (dBm) at the receiver terminal.

Fig.3.18 Plots of penalty in signal power due to Self-phase-modulation & fibre chromatic dispersion at $BER=10^{-9}$ versus power input with bit rate $Br=10$ Gb/s, dispersion co-efficient $D_c=-15$ ps/km-nm, band width $B_{IF}=2$ and modulation index $h=1.0$ for different lengths $L=40$ km, 60km, 80km, 120km at a heterodyne CPFSK receiver.

Fig.3.19 Plots of penalty in signal power due to Self-phase-modulation & fibre chromatic dispersion at $BER=10^{-9}$ versus power input with bit rate $Br=10$ Gb/s, dispersion co-efficient $D_c=-15$ ps/km-nm, band width $B_{IF}=2$ and modulation index $h=0.5$ for different lengths $L=40$ km, 60km, 80km, 120km at a heterodyne CPFSK receiver.

Fig.3.20 Plots of penalty in signal power due to Self-phase-modulation & fibre chromatic dispersion at $BER=10^{-9}$ versus power input with bit rate $Br=10$ Gb/s, dispersion co-efficient $D_c=15$ ps/km-nm, band width $B_{IF}=2$ and modulation index $h=1.0$ for different lengths $L=40$ km, 60km, 80km, 120km at a heterodyne CPFSK receiver.

Fig.3.21 Plots of penalty in signal power due to Self-phase-modulation & fibre chromatic dispersion at $BER=10^{-9}$ versus power input with bit rate $Br=10$ Gb/s, dispersion co-efficient $D_c=15$ ps/km-nm, band width $B_{IF}=2$ and modulation index $h=0.5$ for different lengths $L=40$ km, 60 km, 80 km, 120km at a heterodyne CPFSK receiver.

Fig3.22 Variation of the bit error rate (BER) performance due to different values of Length (say, $L=40,80$ km) of a heterodyne CPFSK receiver at a bit rate 10 Gb/s with fibre chromatic dispersion $D_c=15$ ps/km-nm, band width $B_{IF}=2$, for several values of received power P_s .

Fig.3.23 Variation of power penalty in signal power due to combined effect of Self-phase-modulation & fibre chromatic dispersion at $BER=10^{-9}$ versus modulation index (h) with fibre length $L=40$ km, $Br=10$ Gb/s, dispersion co-efficient $D_c=15$ and band width $B_{IF}=2$ for different values of input power $P_{in}=-10, 0, 15$ dBm for a heterodyne CPFSK receiver.

Fig.3.24 Variation of power penalty in signal power due to combined effect of Self-phase-modulation & fibre chromatic dispersion at $BER=10^{-9}$ versus modulation index (h) with fibre length $L=80$ km, $Br=10$ Gb/s, dispersion co-efficient $D_c=15$ and band width $B_{IF}=2$ for different values of input power $P_{in}=-10, 0, 15$ dB for a heterodyne CPFSK receiver.

Fig.3.25 Comparison between analytical results with the penalty measured from eye-opening by simulation for fibre length $L=30$ km and 50 km at $BER=10^{-9}$, $Br=10$ Gb/s, dispersion coefficient $D_c=15$ ps/km-nm and modulation index $h=1.0$ for direct detection CPFSK receiver.

LIST OF PRINCIPAL SYMBOLS

α	Attenuation (dB/km)
γ	Chromatic dispersion index
τ	Delay occurred due to path difference in MZI
χ	Fibre nonlinear coefficient
ν	Frequency of optical carrier
λ	Optical wavelength
$\Delta\nu$	Normalized linewidth of transmitting laser
$\delta(t)$	Delta function of time
σ^2	Noise variance
η_{eff}	Effective refractive index of MZI
Δf	Frequency deviation of FSK signal
ϕ_i	Angle modulation of i th channel
ϕ_{in}	Phase noise of transmitting laser of i th Channel
ϕ_k	Angle modulation of k th channel
ΔL	Path difference of MZI
ϕ_{out}	Output phase
B	Normalized bandwidth of LP filter
B_2	Dispersion coefficient (ps^2/km)
B_{IF}	Bandwidth of IF filter
B_r	Bit rate
c	Velocity of light
$D(\lambda)$	Fibre Chromatic Dispersion
F	Fourier transform
F^{-1}	Inverse Fourier transform
f_c	Optical carrier frequency
h	Modulation index
$H(f)$	Optical fibre transfer function

$I(t)$	Modulating signal
l_1, l_2	Lengths of arms I and II of MZI
$n(t)$	Complex additive Gaussian noise
N_{c-sp}	Crosstalk noise power
N_{s-sp}	Signal spontaneous noise power
N_{sp}	Spontaneous emission factor
N_{sp-sp}	Spontaneous spontaneous noise power
$P(\Delta\theta_n)$	PSD of $\Delta\theta_n$
P_{in}	Input optical signal power
P_o	Fibre output
P_s	Received optical signal power
R_d	Photon responsivity
S_{pd}	Photo-detector shot noise
S_{pdi}	Interferometric noise
S_{th}	Receiver thermal noise
T_I, T_{II}	Transmittance of arms I and II of MZI

LIST OF ABBREVIATIONS

ASK	Amplitude shift keying
APD	Avalanche photo diode
ASE	Accumulated spontaneous emission
BER	Bit error rate
CPFSK	Continuous phase FSK
dBm	Decible relative to 1 mw
DFB	Distributed feedback
EDFAs	Erbium doped fibre amplifiers
erfc	Complimentary error function
FM	Frequency modulation
FP	Fabry Perot
FSK	Frequency shift keying
FDM	Frequency division multiplexing
FWM	Four wave mixing
GVD	Group velocity dispersion
IF	Intermediate frequency
IM/DD	Intensity modulation direct detection
ISI	Inter-symbol interference
LASER	Light amplification by stimulated emission of radiation
LD	Laser diode
LED	Light emitting diode
LO	Local oscillator
LW	Linewidth
MSK	Minimum shift keying
MZI	Mach-Zehnder interferometer
NRZ	Non-return to zero
OOK	On-off keying
OFD	Optical frequency discriminator

OFDM	Optical frequency division multiplexing
OTDM	Optical time division multiplexing
PDF	Probability density function
PIN	Positive intrinsic negative
PSD	Power spectral density
SNR	Signal to noise ratio
SPM	Self-phase Modulation
WDM	Wavelength division multiplexing

CHAPTER-1

Introduction



1.1 Introduction to optical communication :

The last three decades have witnessed a spectacular progress in the field of optical fibre communications, lasers, optoelectronic devices and technology, in the development of semiconductor laser amplifiers and Erbium doped fibre amplifiers (EDFA) which enabled repeaterless transmission distance of more than 1000 km at a bit rate of 10 Gb/s.

Optical communication utilizes optical signal as the carrier. In optical communication system electrical signals are first converted into optical or light signals by modulating an optical source, such as light emitting diode (LED) or laser diode (LD). Then the optical signal is transmitted over long distances via optical fibre. At the receiving end the optical signal is converted to electrical signal by avalanche photodetector (APD) or PIN photodetector followed by a receiver.

Optical fibre communication system has the following advantages by virtue of its characteristics :

- Low losses: It enables to reduce the number of repeaters;
- High bandwidth: Low cost per channel can be achieved;
- Small bulk: Requires less space;
- Light weight: Lightened the cable;
- Flexibility: Easy to install;
- Resistant to radiation: Less costly protection is required;
- Immunity to radio interference: Increased reliability;

- Difficult to intercept: Security is ensured;
- No conductor: Adequate electrical insulation is assured;

Optical communication system utilizes the infra-red portion of the frequency spectrum. Since the information in the optical carrier frequency is of the order of 10^{14} Hz, which is 10^5 times higher than microwave frequency, optical communication provides higher information capacity and hence leads to improved system performance. Due to dielectric nature of the fibre, optical systems are virtually immune to crosstalk and electro-magnetic interference (EMI), unlike co-axial cables and microwave links. Due to its simplicity and economy in raw materials, low cost, low loss, smaller in size, lighter in weight and flexible in construction, it is considered to be the best transmission media in communication field. From the mentioned advantages, research activities around the world was encouraged in optical fibre communications during the last three decades.

With the invention of LASER in 1960, optical fibre transmission was immediately recognized and efforts in optical communication began. During the last three decades, the increasing development in this field has made optical communication more popular and useful one.

The period of 1965-75 was devoted to the development of graded index fibre system which utilized wavelength of 850-900 nm and achieved information rates in the range of 8-140 Mbit/s. In 1978, research started for single mode fibre technology and it led to the establishment of 1300 nm range single mode fibre system and present trends towards 1500 nm range fibre for long haul system. By 1980s, these activities had led to the development and worldwide installations of practical and economically feasible optical fibre communication systems that carry telephone, cable TV and other types of telecommunication traffics. The principal motivations behind each new one were either to improve the transmission fidelity

and to increase the data rate, so that more information could be sent or to increase the transmission distance between relay stations.

Main components of an optical communication system as shown in Fig. 1.2 are

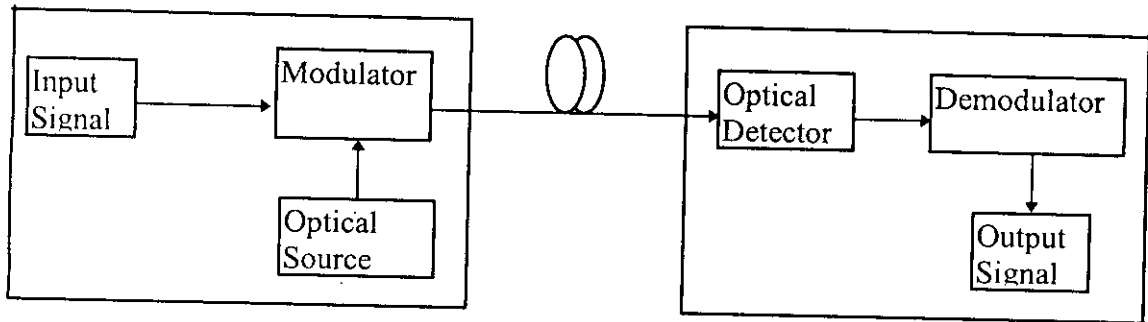


Fig. 1.2 Generalized block diagram of an optical communication system.

- Optical source
- Modulator
- Transmission Media
- Optical detector
- Demodulator

In lightwave communication system, two important detection techniques are normally employed:

- (i) Direct detection
- (ii) Coherent detection

In direct detection, the intensity of the received optical field is directly converted to a current by a photodetector whereas in coherent detection, the received optical field is combined with the light output from a local oscillator (LO) laser and the mixed optical field is converted to an intermediate frequency (IF) signal by heterodyne or directly to base band by homodyne. The first optical communication system employed intensity modulated direct detection (IM/DD) technique and in spite of a lot of research, this scheme is still popular for commercial application due to its low cost and simplicity. However, DD technique has limitation of data rate for application in power limited free-space optical channels due to relatively low optical power output of semiconductor laser diode. To increase the data rate throughput of all-semiconductor free space optical channels, extensive research for bandwidth and power efficient coding and modulation schemes were carried out in the last decade [1-6]. DD optical communication systems are very promising for future deep space applications, inter-satellite links and terrestrial line-of-sight communications.

Coherent optical transmission systems using heterodyne or homodyne are attractive due to their improved receiver sensitivity compared to IM/DD systems and enhanced frequency selectivity in optical frequency division multiplexing (OFDM) system[5]. In coherent optical communication system, information can be impressed on the optical carrier in one of the three ways: (i) phase shift keying (PSK) (ii) frequency shift keying (FSK) or (iii) amplitude shift keying (ASK). Depending on the specific application various modulation and demodulation formats similar to those of traditional radio frequency communication are also employed in coherent light wave transmission. These include: binary PSK (BPSK) quadrature PSK (QPSK), orthogonal QPSK (OQPSK), continuous phase FSK (CPFSK), discontinuous phase FSK (DPFSK), pulse position modulation (PPM) etc. Each of the modulation schemes viz. ASK, FSK, DPSK etc. and combinations thereof, with homodyne, heterodyne or diversity receivers has its own merits and demerits and none has emerged as absolutely preferable. However, FSK systems

are more promising than ASK or PSK due to several reasons. First, modulation can be easily performed using direct modulation characteristic of laser diode (LD) through its injection current [2-4,6]. FSK is flexible enough to allow generation of either compact spectra, which is advantageous in multi-channel OFDM or two-lobe spectra which allows for receiver envelop detection by properly selecting the modulation index. Further, a laser FM transmitter and a receiver front-end can easily be converted to encompass subcarrier modulation scheme, such as MSK-FM for instance and subcarrier multiplexing .

The enormous bandwidth of the optical fibre can be utilized when hundreds of channels can be multiplexed over a single fibre. Optical frequency division multiplexing (OFDM) networks have an ultra large transmission capacity potential [5]. To increase the number of multiplexed channel the signals should be spaced densely. A sharp cut-off filter and a modulation scheme with a compact spectrum are necessary to construct densely spaced multiplexing systems utilizing a direct detection scheme. A periodic filter that consists of an anti-symmetric Mach-Zehnder Interferometer (MZI) is promising because it can multiplex/demultiplex optical carrier with channel spacing in the order of GHz [7]. An FSK scheme has a compact spectrum. A tunable Fabry-Perot filter (FPF) that functions as a channel selective filter is useful for frequency division multiplexed FSK signals and acts as an optical frequency discriminator (OFD). However, a MZI that can act both as modulator/demodulator is more promising as it is 3 dB more power efficient compared to FPF. The periodic filter which consists of anti-symmetric MZI, also functions as a channel selective filter and OFD. When it is used as an OFD, 'mark' and 'space' are differentially detected with two outputs from OFD.

An experiment employing 10 Gbit/s modulation using a III-IV semiconductor MZI has been reported recently [8] and an FDM transmission experiment is also reported with Ghz channel spacing using eight channel tunable demultiplexer [9].

1.2 Limitations of optical fibre communications :

In spite of several advantages, there are some limitations of optical fibre communication systems due to the following effects [10-24].

- (i) Stimulated Raman Scattering (SRS)
- (ii) Stimulated Brillouin Scattering (SBS)
- (iii) Cross-phase Modulation (XPM)
- (iv) Four wave mixing (FWM)
- (v) Chromatic dispersion or Group velocity dispersion (GVD)
- (vi) Laser phase noise
- (viii) Optical amplifier's spontaneous emission (ASE) noise.
- (ix) Self-phase modulation (SPM)

Stimulated Raman Scattering is an interaction between light and vibrations of silica molecules and causes attenuation of short wavelength channels in wavelength-multiplexed systems [10-11]. Stimulated Brillouin Scattering is an interaction between light and sound waves in fibre and causes frequency conversion and reversal of the propagation direction of light [11-13]. Cross-phase modulation (XPM) is an interaction, via the nonlinear refractive index between the intensity of one lightwave and the optical phase of other light waves [14]. Four wave mixing (FWM) is analogous to third order intermodulation distortion whereby two or more optical waves at different wavelengths mix to produce new waves at other wavelength [10-11, 13-15]. Stimulated Brillouin Scattering (SBS) and FWM processes are likely to impose severe restrictions on transmitter power in FDM system.

Fibre chromatic dispersion, laser phase noise, relative intensity noise etc. are other limitations [16-19]. The impulses of various wavelength travel at different speeds through the optical fibre and at the output the impulses get widening. Thus widening of the impulse depends on the spectral width of the source. This effect is

known as chromatic dispersion. If the bit rate increases i.e. time slot decreases the impulses will overlap and no longer be distinguished from each other generates ISI effect, thus limiting transmission bit rate. The amount of dispersion is directly proportional to the fibre length. Chromatic dispersion results in limiting of the fibre transmission capability, due to variation in propagation time as a function of wavelength. This limitation may be overcome to some extent by using a narrower spectrum laser.

Progress in the development of optical amplifiers has made rapid strides in the past few years as the potential advantages have become more obvious and the technology has improved [20-23]. The particular advantages that appeals to system planners is the promise of transparent systems using linear optical repeaters. Such systems can be upgraded in capacity at some future date without any modification of the repeaters. Currently semiconductor laser amplifiers are the most developed and have already been demonstrated in installed optical systems. Development programs have in hand to optimise laser structures for amplifier applications and the initial results have been reported in the past years. The Erbium-doped amplifier cascades provide gain but they also introduce amplified spontaneous emission (ASE) noise which beats with itself, signal and other channels passing through the filter [24]. The limitation of cascaded in-line amplifier systems are recently reported experimentally taking into considerations the effects of linear ASE accumulation [25].

1.3 Brief review of previous works :

To meet higher transmission capacity in exchange network, there is increasing interest in optical fibre transmission at 10 Gbit/s or more. A sufficient amount of research works have been reported which encounters the degrading effects of laser phase noise, nonuniform FM response of DFB laser, nonlinear effects of optical fibre etc. on coherent and direct detection optical transmission systems. A number

of nonlinear fibre effects are now being widely studied; for example, self phase modulation (SPM), four wave mixing (FWM), cross phase modulation (XPM), stimulated Brillouin scattering (SBS) and stimulated Raman Scattering (SRS).

In many recent studies the problems have been focused regarding the detection performance of a coherent lightwave transmission link which caused sharp degrade by laser phase noise and chromatic dispersion. Recent advances in optical signal transmission have already reached several thousands of kilometers in the Gigabit-per-second range due to use of in-line amplifier in different stages of light wave communication system [26]. The theoretical and experimental results have been reported at 10 Gbit/s with coherent and direct detection receivers with in-line optical amplifiers [20-24]. The limitations of cascaded in-line amplifier systems are recently reported experimentally taking into considerations the effects of linear ASE accumulation [25]. The transmission capacity requirement for optical communication system is increasing to meet the future demands of multimedia services which can be achieved by Optical Time Division Multiplexing (OTDM)[27], Wavelength Division Multiplexing (WDM) [28] and / or their combination.

In single-channel intensity modulated direct detection (IM/DD) optical transmission systems, the interplay between SPM and fiber dispersion is an especially important nonlinear effect, since it distorts the received waveform, degrades receiver sensitivity and limits transmission distance and/or optical amplifier output power [22,29-30]. The performance limitation of IM/DD systems with non-negligible SPM is now being widely studied using transmission experiment and numerical solutions [31] and an analytical approach [32]. Marcuse [22] obtained an expression for the RMS pulse width in cascaded amplifier systems using the average optical power approximation. However, it can only be applicable to the case of weak dispersion. Also, it can only be applicable for the transmission system in which all system parameters, such as fibre dispersion,

amplifier output power and the amplifier spacing, are the same all over the transmission system.

In numerical simulations, the waveform distortion caused by SPM is obtained from numerical solution of the non-linear Schrodinger equation in the transmission fibre by using methods such as the split step Fourier (SSF) method [31]. The numerical approach lacks as analytical equation and physical insight into how SPM affects system performance. That is a complicated and painstaking approach. For example, it is difficult to estimate the change in transmission distance by varying system parameters, such as the number and output power of optical amplifiers, fibre dispersion values and length of each fibre section. Moreover, it is known from the numerical simulation that the amount of waveform distortion to be changed when the distribution of dispersion along the transmission line is changed, but it is difficult to obtain qualitative and quantitative understanding of its mechanism by numerical simulation. Therefore there is an urgent need for an analytical approximation technique of SPM.

An analytical technique has recently been proposed in reference [32] which gives an expression for the root-mean-square (RMS) pulse width of an optical pulse in IM/DD system after non-linear fibre transmission, but it is only applicable to the case without optical repeaters. Analytical approach to evaluate the effects of SPM on optical CPFSK system is very much complicated and are yet to be reported. The results reported on SPM for applying only IM/DD system.

1.4 Objectives of the study :

The main objectives of the present research work are :

- (i) to develop an analytical approach to evaluate the effects of self phase Modulation (SPM) on optical FSK transmission system with two types of receiver configurations, viz. direct detection receiver and heterodyne receiver;
- (ii) to develop a baseband equivalent transfer function of a single mode fibre to represent the effect of Self-phase-modulation (SPM);
- (iii) to develop an expression for the amount of signal phase distortion due to SPM and the received waveform at the fibre output;
- (iv) to determined the moments and probability density function (PDF) of the random phase fluctuation in the receiver output;
- (v) to evaluate the bit error rate (BER) of the receiver by using the statistics of the random phase fluctuations for a given input power and fibre dispersion; and finally
- (vi) to determine, for a given BER of 10^{-9} , the power penalty suffered by the system due to SPM and to estimate theoretical maximum fibre length at a bit rate of 10 Gbit/s for a specified power penalty and the maximum allowable transmitter power input to the fibre.

Chapter- 2

Effect of GVD and SPM on optical CPFSK system

2.1 Overview:

Optical continuous-phase FSK (CPFSK) may be an attractive modulation format for future multichannel coherent optical systems. However, at high bit rate operation of such systems in conventional single-mode fiber, the major limitation is due to the group velocity dispersion (GVD), unless a dispersion compensation scheme is used. Further, fluctuation in signal power due to GVD causes a random phase modulation of the signal itself due to nonlinear refractive index of fibre. The effect is termed as self-phase-modulation (SPM) and causes spectral broadening of the transmitted signal and higher bandwidth requirement and degrades receiver performance. The effect of SPM is directly proportional to the signal power input to the fibre and the fibre length. At increased signal power the effect is much more pronounced and imposes severe restrictions on the maximum allowable signal power input to the fibre and hence maximum repeaterless transmission distance.

Theoretical performance analysis of optical CPFSK & DPSK systems with direct detection receiver have been carried out recently considering the effect of GVD only [33-34]. For an intensity modulated direct detection system (IM-DD), the pulse broadening due to group velocity dispersion (GVD) causes intersymbol interference (ISI) and an estimate of the dispersion penalty is theoretically reported recently [18]. For coherent angle-modulated optical systems the analytical results for dispersion penalty are not widely available in the literature. However, the work reported in [18] based on numerical simulation and provides useful results on dispersion penalty in terms of the eye-penalty. The eye-closure penalty is an approximate measure of the system performance degradation but not an accurate measure because of its limitations.

The simulation results on the effect of SPM on optical IM/DD system are discussed in Ref.[31] where the penalty estimates are made for eye-openings at the fibre output. The analytical approach to evaluate the effect of SPM on the performance of intensity modulated direct detection (IMDD) system is recently reported [32] where the effect of SPM is estimated by an α -parameter estimation of the Gaussian pulse shape of the on-off optical pulses. The effect of SPM on angle-modulated system is much more complicated and not yet reported. Because of the inherent complexity in the analytical approach, the performance degradations due to GVD only is reported in terms of the eye-closure penalty, utilizing the standard simulation approach [18]. The results are mostly pattern specific and rely mostly on eye-closure due to signal degradation. Therefore, the conclusions reached are without the consideration of accompanying noise and knowledge of the exact receiver output statistics. For an accurate system design an analytical evaluation of the system penalty is much desired.

In this chapter we provide an analytical evaluation method to evaluate the performance limitations of Self-phase-modulation on an optical CPFSK system. The analysis also includes the effect of GVD and laser phase noise. The method is based on the linear approximation of the output phase of a linearly filtered angle-modulated signal such as the CPFSK signal considered in this thesis work. An equivalent transfer function of a single mode fibre is derived which includes the effects of SPM in presence of GVD. The overall degradation in signal phase is also derived following by analytical approach. The expression for BER is then derived considering the effects of GVD & SPM in presence of laser phase noise and receiver noise. The analysis is carried out for both direct detection receiver and heterodyne delay demodulation receiver.

2.2 System Model :

2.2.1 Direct Detection CPFSK :

The schematic diagram of an optical CPFSK system using direct detection receiver configuration is shown in Fig. 2.1. In the transmitter, non-return-to-zero (NRZ) data at 10 Gb/s is used to directly modulate a laser to generate the CPFSK signal which is transmitted through a single-mode fibre. At the receiving end, the received optical signal is detected by a Mach-Zehnder interferometer based direct detection receiver.

In the FSK direct detection receiver with MZI the MZI acts as an optical filter and differentially detects the 'mark' and 'space' of received FSK signal which are then directly fed to a pair of photodetectors. The difference of the two photocurrents are applied to the amplifier which is followed by an equalizer. The equalizer is required to equalize the pulse shape distortion caused by the photodetector capacitance and due to the input resistance and capacitance of amplifier. After passing through the baseband filter, the signal is detected at the decision circuit by comparing it with a threshold of zero value.

One other type of discriminator is the Fabry-Perot etalon Interferometer; a small comparison in connection to direct detection would reveal some relevant aspects.

1. Mach-Zehnder Interferometer and Fabry-Perot etalon Interferometer both can act as tunable filter (for multichannel application) and optical discriminator.
2. The OFDs (MZI/FPI) are built with passive components which are less costly compared to heterodyne system.
3. MZI provides easy tunability in multichannel system compared to heterodyne system which requires LDs with wide tuning range and narrow LW.
4. Receiver design is simple and less costly due to the absence of the sophisticated wideband IF circuits.

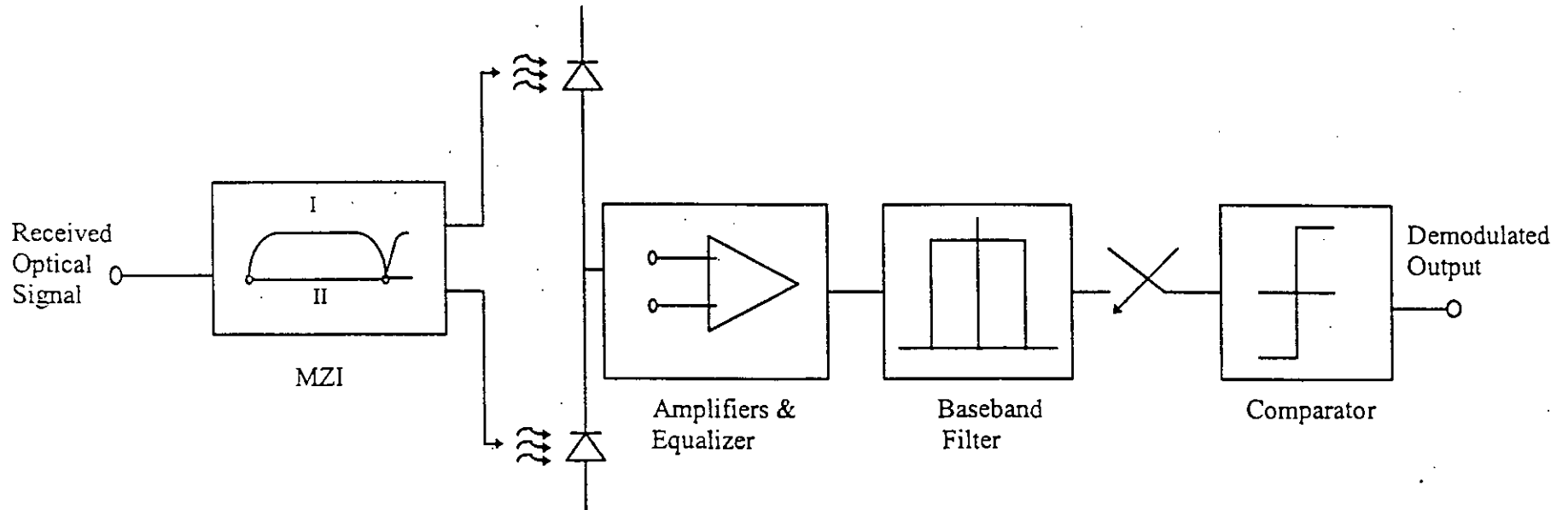


Fig. 2.1 Block diagram of an FSK direct detection receiver with Mach-Zehnder Interferometer (MZI) as an optical frequency discriminator (OFD).

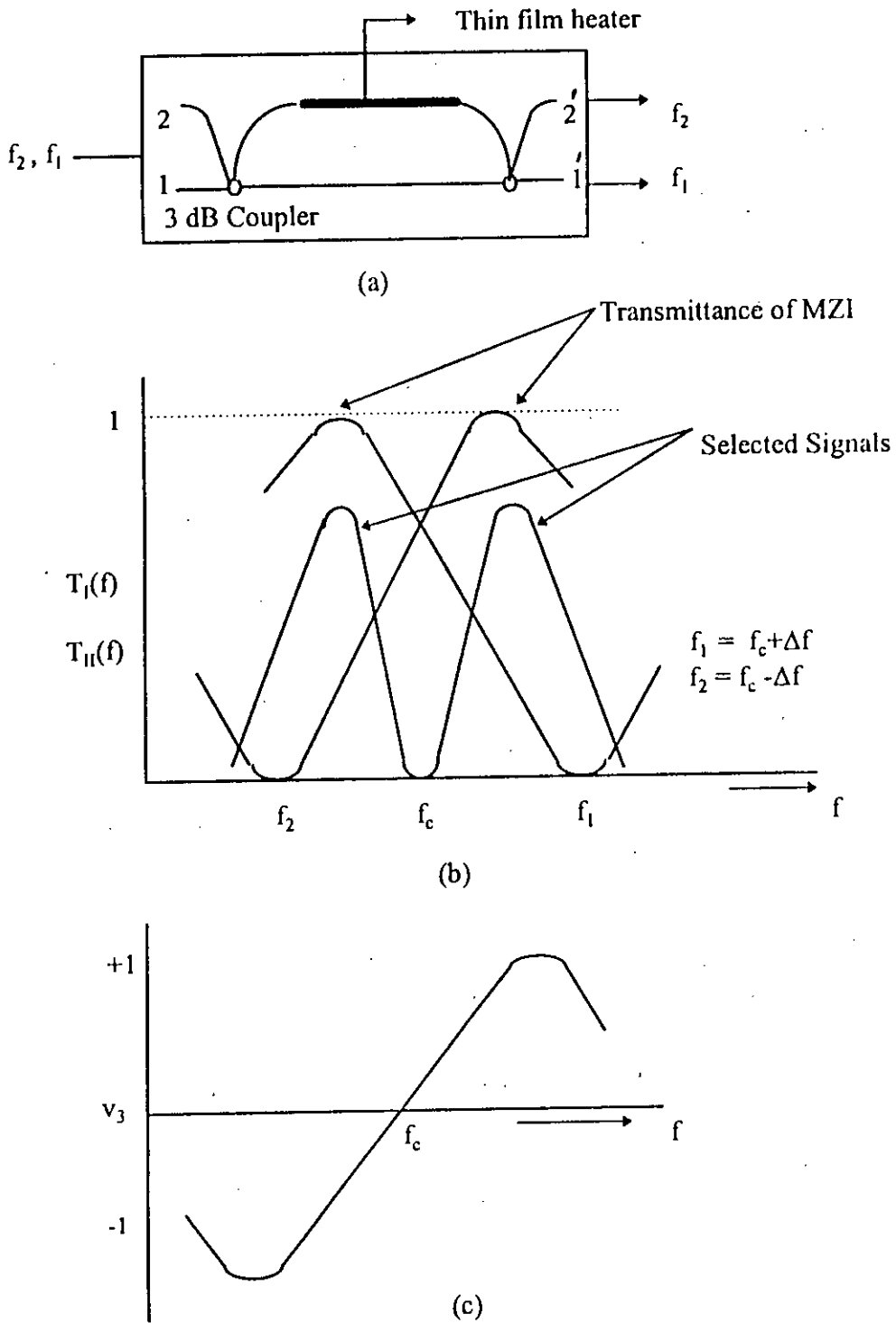


Fig.2.2 (a) An MZI with large ΔL or narrow wavelength spacing,
 (b) Transmittance characteristics of an MZI and
 (c) Differential output of the balanced receiver.

2.2.2 Operation of MZI :

It is a common property of the interference filters to transmit a narrow band of wavelength and blocking all wavelengths outside the band. In our receiver, MZI is employed which is integrated with a silica waveguide. It is a very promising device in wavelength division multiplexing (WDM) and frequency division multiplexing (FDM) systems. Because of their high frequency selectivity without mechanical actuator (which is essential for an FPI), MZIs can be series cascaded to achieve increased transmission capacity[7].

MZI has two input ports, two output ports, two 3 dB couplers and two waveguide arms with length difference ΔL . A thin film heater is placed in one of the arms to act as a phase shifter, because light path length of heated wave guide arm changes due to the change of refractive index. The phase shifter is used for precise frequency tuning. Frequency spacing of the peak to bottom transmittance of the OFD is set equal to the peak frequency deviation $2\Delta f$ of the FSK signal. Consequently, the 'mark' and the 'space' appear at the two output ports of the OFD. These outputs are differentially detected by the photodetectors with balanced configuration.

2.2.3 MZI Characteristics :

If $E(t)$ represents the signal input to the MZI, then the signals received at the output ports can be expressed as [8]

$$|E_2(t)| = |E(t)| \sin \left[\frac{k(l_2 - l_1)}{2} \right] \quad (2.1)$$

and

$$|E_1(t)| = |E(t)| \cos \left[\frac{k(l_2 - l_1)}{2} \right] \quad (2.2)$$

where l_1 and l_2 are the length of two arms of MZI and k is the wave number which can be expressed as

$$k = \frac{w}{v} = \frac{2\pi}{\lambda} = \frac{2\pi f \eta_{eff}}{c} \quad (2.3)$$

η_{eff} , f and c are the effective refractive index of the wave guide, frequency of optical input signal and velocity of light in vacuum, respectively.

The transmittance of arm II of MZI is given by

$$T_{II}(f) = \frac{|E_2(t)|^2}{|E(t)|^2} = \sin^2 \left[\frac{k(l_2 - l_1)}{2} \right] = \sin^2 \theta \quad (2.4)$$

and that of arm I of MZI is

$$T_I(f) = \frac{|E_1(t)|^2}{|E(t)|^2} = \cos^2 \left[\frac{k(l_2 - l_1)}{2} \right] = \cos^2 \theta \quad (2.5)$$

where, θ is the phase factor related to the arm path difference $\Delta L = l_2 - l_1$ and can be expressed as

$$\theta = \frac{k\Delta L}{2} = \frac{\pi f \eta_{eff} \Delta L}{c} \quad (2.6)$$

Normally ΔL is chosen as

$$\Delta L = \frac{c}{4\eta_{eff} \Delta f} \quad (2.7)$$

Therefore,

$$\theta = \frac{\pi f}{4\Delta f} \quad (2.8)$$

Then we get

$$T_{II}(f) = \sin^2\left(\frac{\pi f}{4\Delta f}\right) \quad (2.9)$$

and

$$T_I(f) = \cos^2\left(\frac{\pi f}{4\Delta f}\right) \quad (2.10)$$

The outputs of the MZI are, therefore, anti-symmetric and are shown in Fig. 2.2

For an MZI used as an OFD, Δf is so chosen that $\Delta f = \frac{f_c}{2n+1}$, f_c is the carrier frequency of the FSK signal and n is an integer. The 'mark' and 'space' of FSK signals are represented by f_1 and f_2 respectively where $f_1 = f_c + \Delta f$ and $f_2 = f_c - \Delta f$.

Therefore, when 'mark' (f_1) is transmitted

$$T_I = 1 \text{ and } T_{II} = 0$$

Similarly, for transmission of 'space'

$$T_I = 0$$

$$\text{and } T_{II} = 1$$

Thus, two different signals f_1 and f_2 can be extracted from two output ports of MZI.

The MZI is used in our analysis only as an OFD as our analysis is based on single channel operation. The complete potential of an MZI can be extracted when a multiplexer/ demultiplexer or a frequency selection switch for a multi channel WDM/ FDM system is fabricated utilizing the periodicity of the transmittance versus frequency characteristic of an MZI.

2.3 Theoretical analysis for DD-CPFSK :

The complex envelope of the electric field at the output of CPFSK transmitter and input envelope of the fibre is represented as

$$E_{in} = \sqrt{2P_T} \exp[(j\phi_{in}(t))] \quad (2.11)$$

where P_T is the average transmitted power and the angle modulation $\phi_{in}(t)$ is given by

$$\phi_{in}(t) = 2\pi\Delta f \int_{-\infty}^t \sum_{k=-\infty}^{\infty} a_k p(t-kT) dt + \phi_n(t) \quad (2.12)$$

with $a_k = \pm 1$ representing the k th information bit, $p(t)$ is a unit rectangular pulse of duration T seconds (bit rate $B=1/T$), Δf is the frequency deviation ($h=2\Delta fT$, is the modulation index) and $\phi_n(t)$ is the instantaneous phase noise of the transmitting laser.

Utilizing PM-AM conversion induced by GVD [32] and the resulting generated SPM, the Fourier transform of the output phase $\phi_{out}(\omega)$ and the output power fluctuation $\xi_{out}(\omega)$, under linear phase approximation [35], are related to the corresponding transforms of the input quantities viz. $\phi_{in}(\omega)$ and $\xi_{in}(\omega)$, through a transfer function matrix :

$$\begin{bmatrix} \phi_{out}(\omega) \\ \xi_{out}(\omega) \end{bmatrix} = B_{SPM}(N, \omega) \begin{bmatrix} \phi_{in}(\omega) \\ \xi_{in}(\omega) \end{bmatrix} \quad (2.13)$$

where, $B_{SPM}(N, \omega)$ is the transfer function of a system of N cascaded segments each of length L_k . Corresponding to an input phase excitation $\phi_{in}(t)$, the output phase response $\phi_{out}(t)$ can be directly obtained from eqn.(2.13). By virtue of the validity of linear phase approximation in a practical situation, we introduce an equivalent phase impulse response $h(t) = F^{-1}[B_{SPM}(N, \omega)]$ where the 2×2 matrix $B_{SPM}(N, \omega) = G_N A_N(\omega) \dots G_1 A_1(\omega)$, G_i is a gain matrix of the i -th amplifier and F^{-1} denotes the inverse Fourier transform.

The matrix A_k can be formed as : $A_k = \lim_{q \rightarrow \infty} A^q \dots A^p \dots A^{-1}$, and the matrix A^p is given by

$$A^p = \begin{bmatrix} \cos(\omega^2 F_k) & -2P_0 e^{-p\alpha\Delta L_k} \sin(\omega^2 F_k) \\ \frac{e^{p\alpha\Delta L_k} \sin(\omega^2 F_k)}{P_0} + \chi\Delta L_k & \cos(\omega^2 F_k) \end{bmatrix} \quad (2.14)$$

$$\text{where, } F_k = \beta_2^k \Delta L_k / 2 \quad (2.15)$$

and β_2^k is the dispersion coefficient in ps^2/km in the k-th segment, χ is the fibre nonlinear coefficient, P_0 is the signal power input to the fibre, α is the fibre attenuation, and $\Delta L_k = L_k / q$.

The complex envelope of the electric field at the fibre output is then obtained as

$$E_{out} = F^{-1} [E_{in}(f)H(f)] = \sqrt{2P_s} \exp[j\phi_{out}(t)] \quad (2.16)$$

where F^{-1} denotes the inverse Fourier transform, P_s is the average received power and the output phase $\phi_{out}(t)$ is [35]

$$\phi_{out}(t) = \text{Re}[\phi_{in}(t) * h(t)] + \sum_{n=2}^{\infty} \frac{1}{n!} \text{Im}(j^n f_n) = \phi_{lin}(t) + \phi_{im}(t) \quad (2.17)$$

where Re and Im denote the real and imaginary parts respectively, $h(t)$ is the complex 'impulse response' of the fibre and the explicit expressions for $f_n(t)$ can be found in [35]. Equation (2.17) simply states that the output phase is the sum of a linear term, $\phi_{lin}(t)$ that represents linear filtering of the input phase and a nonlinear distortion term $\phi_{im}(t)$. We define the mean-square phase error as

$$MSE = E[\phi_{out}(t) - \phi_{lin}(t)]^2 / E[\phi_{lin}^2(t)] \quad (2.18)$$

The output phase $\phi_{out}(t)$ can be closely approximated by $\phi_{lin}(t)$ if $MSE \ll 1.0$ [36]. Figure 2.3 depicts the MSE against γ for CPFSK ($h=1$) and MSK ($h = 0.5$) obtained by simulation. As seen, the linear phase approximation is quite accurate for practical usable range of values of γ .

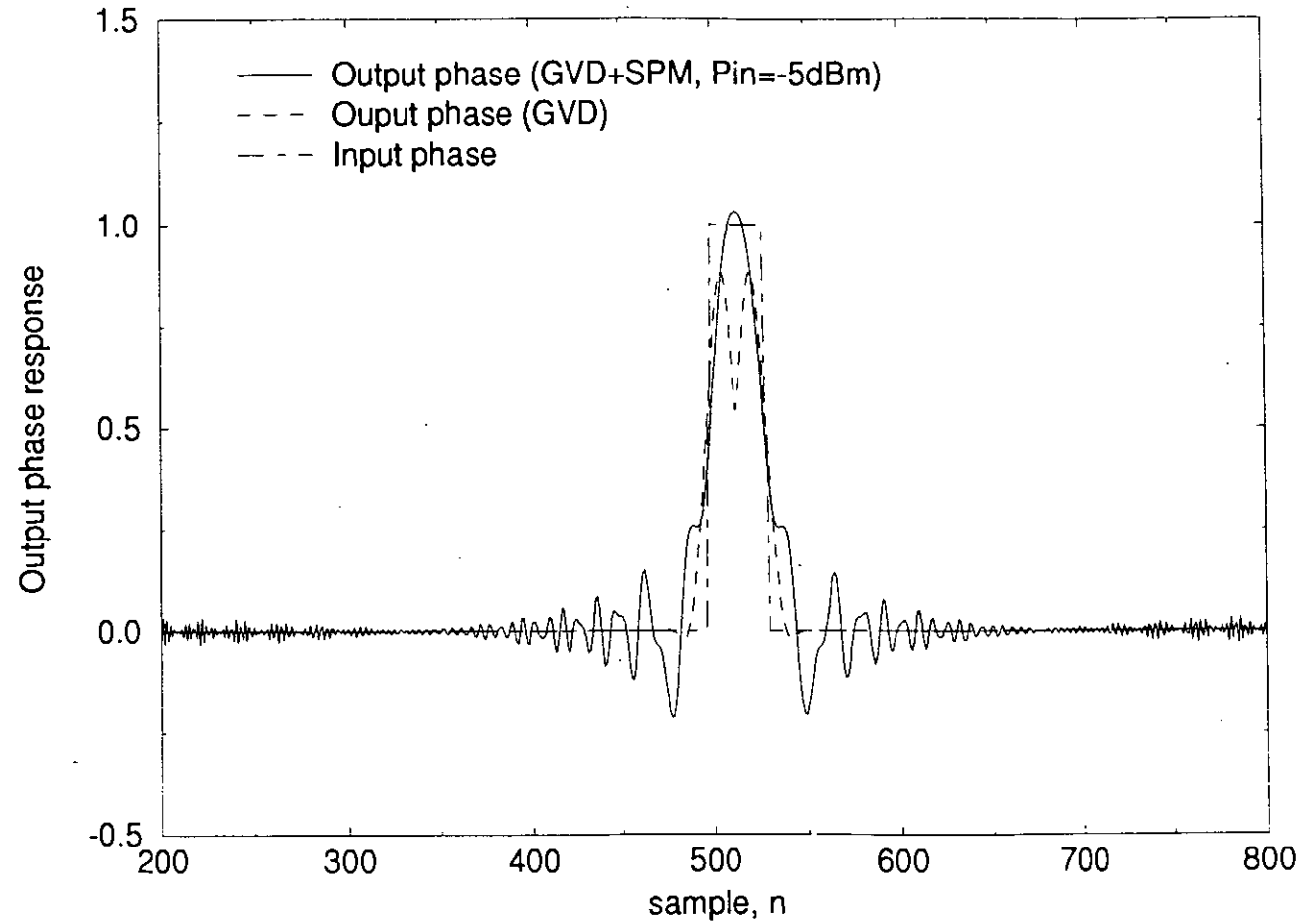


Fig.2.3 Output phase response of single mode fibre for rectangular input phase with fibre span length $L=50\text{ km}$, $P_{in}=-5\text{dBm}$.

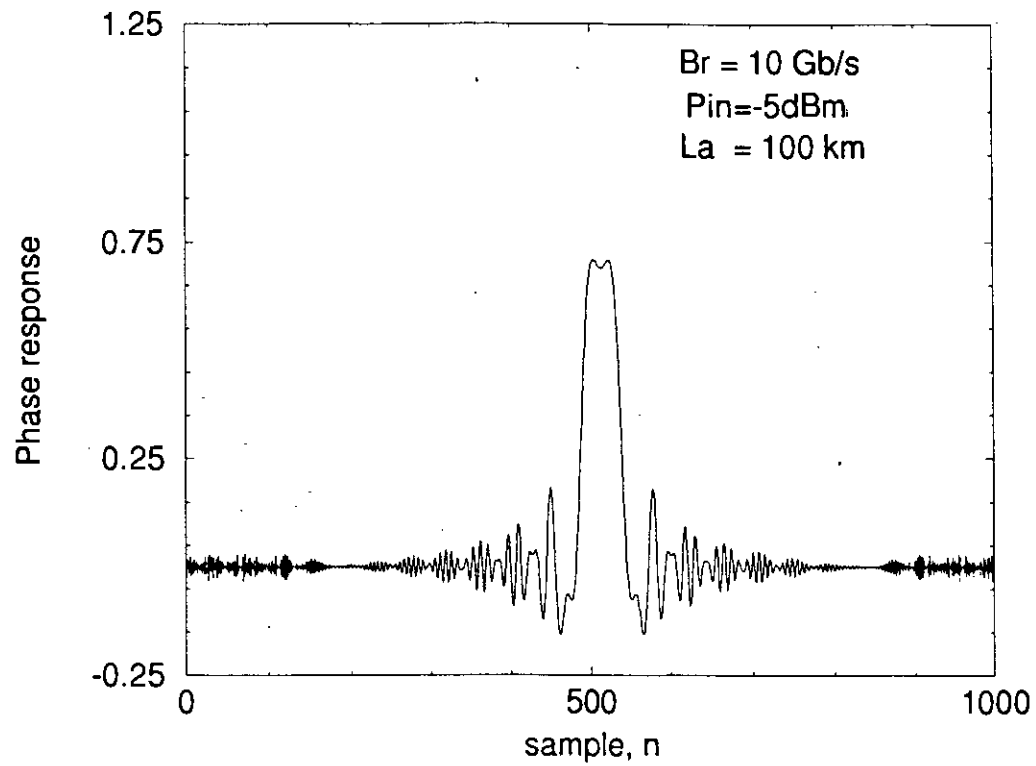


Fig.2.4 (a) Output phase response of single mode fibre for rectangular input phase with fibre span length $L=100$ km, $P_{in} = -5$ dBm.

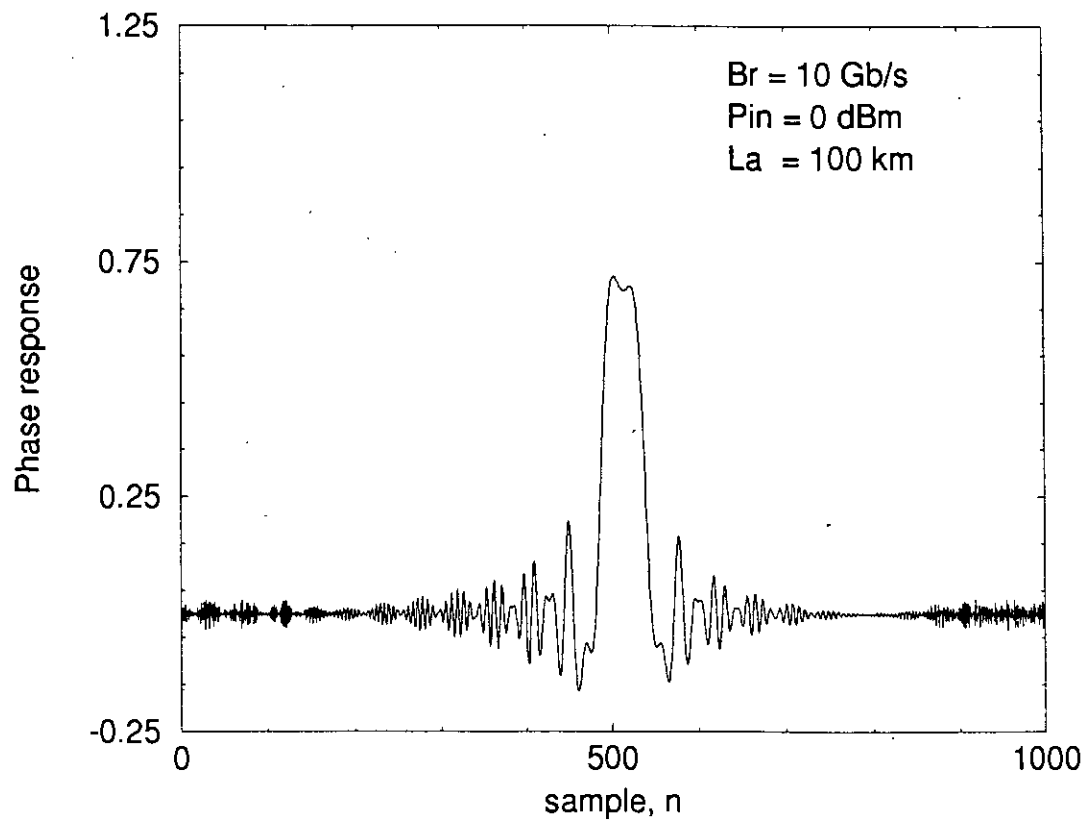


Fig.2.4 (b) Output phase response of single mode fibre for rectangular input phase with fibre span length $L=100$ km, $P_{in}=0$ dBm.

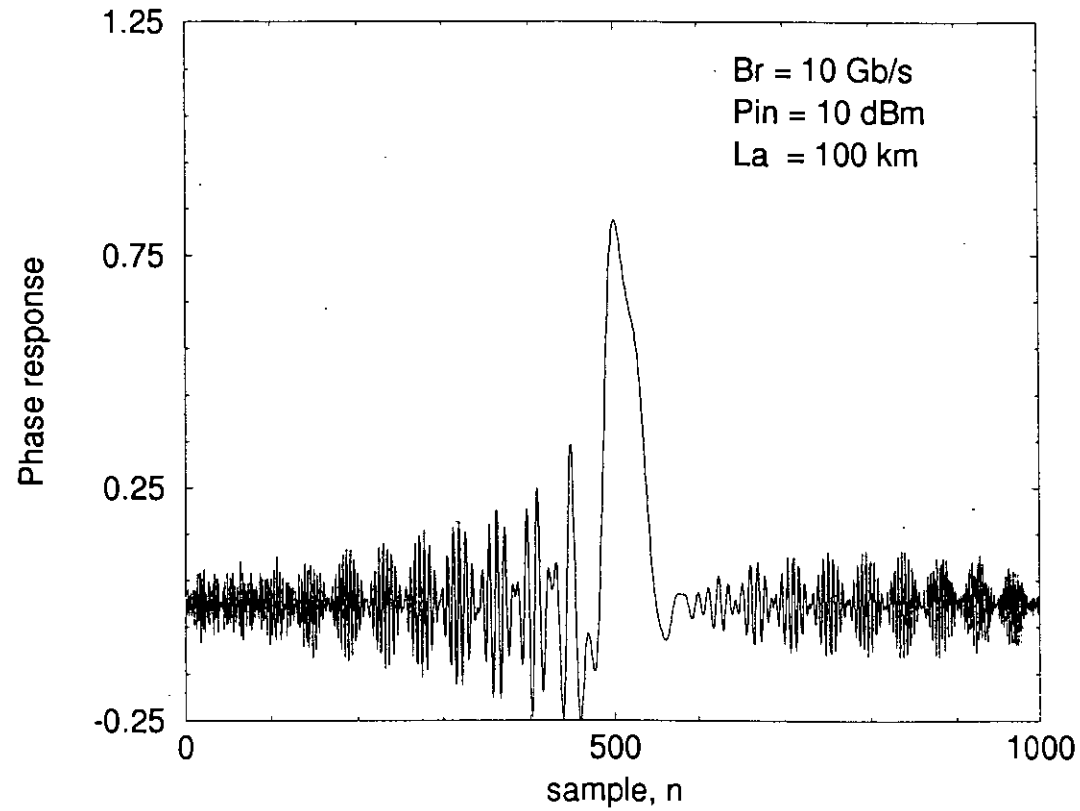


Fig.2.4 (c) Output phase response of single mode fibre for rectangular input phase with fibre span length $L=100$ km, $P_{in}=10$ dBm.

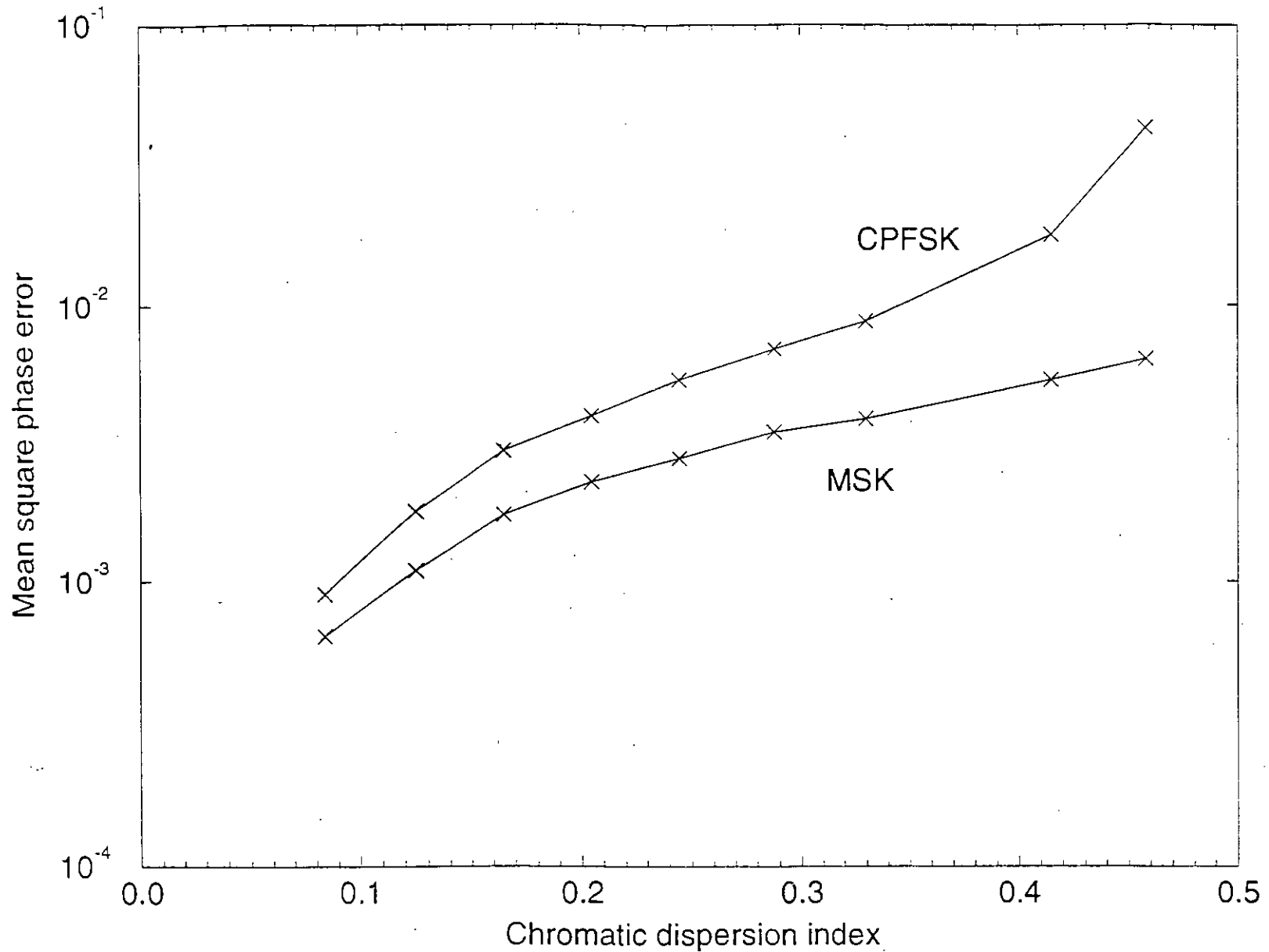


Fig.2.5 Variation of Mean square phase error (MSE) with respect to Chromatic dispersion index γ , for CPFSK ($h=1$) and MSK ($h=0.5$) obtained by simulation.[40]

The optical field at the output of two branches of MZI can now be expressed as :

$$\text{and } E_2(t) = \frac{1}{2}[E(t - \tau_b) - E(t - \tau_a)] \quad (2.19)$$

$$E_1(t) = \frac{-j}{2}[E(t - \tau_a) - E(t - \tau_b)] \quad (2.20)$$

where,

$$\tau_a = \frac{\eta l_1}{c}$$

$$\tau_b = \frac{\eta l_2}{c}$$

Let us define the time delay due to path difference in MZI as

$$\tau = \tau_b - \tau_a = \frac{\eta(l_2 - l_1)}{c} \quad (2.21)$$

Without any loss of generality we can take $\tau_a=0$, then $\tau_b=\tau$. Using equation (2.1), (2.11) and (2.19) the output current of upper photodetector is given by [37].

$$i_2(t) = R_d |E_2(t)|^2$$

$$= \frac{R_d P_s}{2} [1 - \cos\{2\pi f_c \tau + 2\pi \Delta f \int_{t-\tau}^t \sum_k a_k g(t_1 - kT) dt_1 + \Delta\phi_n(t, \tau)\}] \quad (2.22)$$

where, R_d is the responsivity of the photodetector.

Similarly, the output current at the lower photodetector can be expressed as

$$i_1(t) = R_d |E_1(t)|^2$$

$$= \frac{R_d P_s}{2} [1 + \cos\{2\pi f_c \tau + 2\pi \Delta f \int_{t-\tau}^t \sum_k a_k g(t_1 - kT) dt_1 + \Delta\phi_n(t, \tau)\}] \quad (2.23)$$

The output of the balanced photodetectors is then found as

$$i_o = i_1 - i_2$$

$$= R_d P_s \cos[\omega_c \tau + \Delta\phi_s(t, \tau) + \Delta\phi_n(t, \tau) + \phi_0] \quad (2.24)$$

Hence, the balanced receiver output signal current when a 'mark' is transmitted at a sampling time t , is

$$i_m(t) = R_d P_s \cos\left[2\pi f_c \tau + \frac{\pi}{2} - \frac{\pi}{2} + \frac{\pi}{2} q(t) + \frac{\pi}{2} \sum_{k \neq 0} a_k q(t - kT) + \Delta\phi_n(t)\right]$$

where, --- (2.25)

$$q(t) = \frac{1}{\tau} \int_{t-\tau}^t g(t_1) dt_1, \quad (2.26)$$

$$\Delta\phi_n(t) = 2\pi \int_{t-\tau}^t \mu(t_1) dt_1 \quad (2.27)$$

$\mu(t)$ is a zero-mean Gaussian frequency noise of two-sided flat power spectral density (psd) of height $\Delta\nu/2\pi$, $\Delta\nu$ being the transmitting laser linewidth, and $g(t) = \text{Re}[p(t) * h(t)]$. In (2.25) the first two terms in the argument of the cosine function provides the expected phase change for the 'mark' received in an 'ideal' case, the next three terms represent the phase distortion of the signal, $\Delta\phi_s(t)$:

$$\begin{aligned} \Delta\phi_s(t) &= \left[-\frac{\pi}{2} + \frac{\pi}{2} q(t)\right] + \left[\frac{\pi}{2} \sum_{k \neq 0} a_k q(t - kT)\right] \\ &= \overline{\Delta\phi_s} + \Delta\phi_s^r \end{aligned} \quad (2.28)$$

induced by SPM and the last term accounts for the phase distortion due to laser phase noise. In equation (2.28) $\overline{\Delta\phi_s}$ represents the mean phase error and $\Delta\phi_s^r$ represents a random phase fluctuation due to ISI for random data bit pattern caused by the combined influence of SPM and GVD.

Under ideal CPFSK demodulation conditions viz., $2\pi f_c \tau = (2n+1)\pi/2$; (n an integer), and $2\pi \Delta f \tau = \pi/2$ for NRZ data, the output signal currents corresponding to 'mark' and 'space' transmission are then obtained as :

$$i_m(t) = R_d P_s x(t) \text{ and } i_s(t) = -R_d P_s x(t) \quad (2.29)$$

where $x(t) = \cos[\Delta\phi(t)]$ describes interferometric intensity noise due to random phase fluctuations,

$$\text{and } \Delta\phi(t) = \Delta\phi_s(t) + \Delta\phi_n(t) \quad (2.30)$$

Ignoring the low-pass filtering effect on the phase noise dependent signal term, for analytical simplicity, the low-pass filter output for 'mark' transmitted, at a sampling time t is

$$i(t) = R_d P_s \cos[\Delta\phi(t)] + n(t) \quad (2.31)$$

where $n(t)$ is the sample function of the filtered output noise contributed by the photodetector quantum shot noise, the interferometric noise due to input intensity fluctuation and the receiver thermal noise having respectively the spectral densities [37]:

$$S_{pd}(f) = eR_d P_s \quad (2.32)$$

$$S_{pdi}(f) = 0.5R_d^2 P_s^2 [S_x(f) - \bar{x}^2 \delta(f)] \quad (2.33)$$

$$S_{th} = i_{th}^2 \quad (2.34)$$

where $S_x(f)$ and \bar{x} represent the psd and the mean value of $x(t)$ respectively and $\delta(f)$ is a delta function in frequency. Denoting the total noise power spectral density by

$$S_n(f) = S_{pd}(f) + S_{pdi}(f) + S_{th} \quad (2.35)$$

the total noise power at the receiver output can be obtained as

$$\sigma_n^2 = \sigma_s^2 = \int_{-\infty}^{\infty} S_n(f) |H_R(f)|^2 df \quad (2.36)$$

where $H_R(f)$ is the transfer function of a Gaussian low-pass filter in the receiver of 3-dB bandwidth equal to 0.75 B.

Conditioning $\Delta\phi(t)(=\Delta\phi)$ in (2.31) and defining $Q = (i_m - i_s) / (\sigma_m + \sigma_s)$, the conditional bit error rate of direct detection CPFSK receiver is given by [37]

$$P(e|\Delta\phi) = 0.5 \operatorname{erfc}(Q/\sqrt{2}) \quad (2.37)$$

The average bit error rate (BER) of a direct detection CPFSK system can then be

$$\text{obtained as } BER = 0.5 \int_{-\infty}^{\infty} \operatorname{erfc}\left(\frac{Q}{\sqrt{2}}\right) p_{\Delta\phi}(\Delta\phi) d(\Delta\phi) \quad (2.38)$$

where $p_{\Delta\phi}(\Delta\phi)$ is the probability density function (pdf) of $(\Delta\phi)$.

Using the Gauss-quadrature rule [41], the BER can be numerically computed as

$$BER = 0.5 \sum_{i=1}^N \int_{-\infty}^{\infty} \omega_i \operatorname{erfc} \left[\frac{R_d P_s \cos(\Delta\phi_{s,i}^r + \Delta\phi_n)}{\sqrt{2} \sigma_m} \right] p_{\Delta\phi_n}(\Delta\phi_n) d(\Delta\phi_n) \quad (2.39)$$

where the weights ω_i and the nodes $x_i = \Delta\phi_{s,i}^r$ are evaluated from the knowledge of the moments of the random process $\Delta\phi_s^r(t)$. The moments of the random process $\Delta\phi_s^r(t)$ can be evaluated using the following recursive relation [38]

$$M_{2r} = Y_{2r}(N) \quad (2.40)$$

$$Y_{(2r)}(i) = \sum_{j=0}^r ({}^{2r}C_{2j}) Y_{2j}(i-1) q_i^{2r-2j} \quad (2.41)$$

Here N is the actual number of interfering terms in the summation equation (2.25). The pdf of the laser phase noise at the output is Gaussian with zero-mean and variance $\sigma_{ph}^2 = 2\pi\Delta\nu\tau$ [17].

2.4 Theoretical Analysis of Heterodyne CPFSK

The block diagram of the CPFSK transmission system is shown in Fig. 2.4. The input to the fiber is a CPFSK signal whose complex envelop is given by equation (2.11). In the receiver the local oscillator translates the received signal to the intermediate frequency (IF). The IF filter output can be written as

$$v(t) = V_0 a(t) \cos[2\pi f_{IF} t + \alpha_s(t) + \alpha_n(t)] + n(t) \quad (2.42)$$

$$\text{where, } a(t) = \left| \int_{-\infty}^{\infty} g(t') e^{j\phi(t-t')} dt' \right|, \quad g(t) = p(t) * h(t) * h_{IF}(t)$$

where $V_0 = 2R_d \sqrt{P_s P_{lo}}$, P_s is the received power, P_{lo} is the local oscillator power, R_d is the responsivity of the photodiode, f_{IF} is the IF frequency, $n(t)$ is the filtered version of the receiver noise with variance $N_0 = 2eR_d P_{lo} B_{IF}$, e represents the electronic charge, B_{IF} is the IF filter bandwidth.

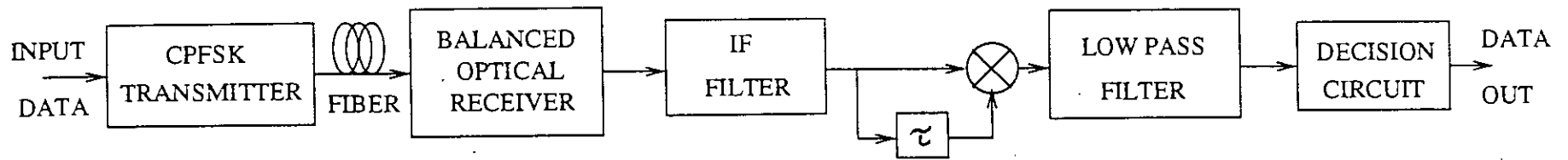


Fig.2.6 Block diagram of an optical heterodyne CPFSK system.

$$\alpha_s(t) = \phi_s(t) * h(t) * h_{IF}(t), \quad (2.43)$$

$$\alpha_n(t) = \phi_n(t) * h(t) * h_{IF}(t), \quad (2.44)$$

and $\phi_n(t)$ is the combined phase noise of the signal and local oscillator lasers at the input of the IF filter and is modelled as a nonstationary Wiener-Levy process [17] and $\phi_s(t)$ is the angle modulation due to the signal given by

$$\phi_s(t) = 2\pi\Delta f \int_{-\infty}^t \sum_{k=-\infty}^{\infty} a_k p(t - kT) dt \quad (2.45)$$

Following delay demodulation (delay time τ) and low-pass filtering (wide enough to pass the signal undistorted), the low-pass filter (LPF) output is given by [39]

$$V_{out}(t) = A(t) \cos[\Delta\phi(t, \tau)] \quad (2.46)$$

where $A(t)$ is the amplitude and the phase of $V_{out}(t)$ can be expressed as

$$\Delta\phi(t, \tau) = 2\pi f_{IF} \tau + \Delta\alpha_s(t, \tau) + \Delta\alpha_n(t, \tau) + \Delta\theta_n(t, \tau) \quad (2.47)$$

Using the notation $\Delta x(t, \tau) = 2\pi \int_{t-\tau}^t x(t_1) dt_1$

and $\theta_n(t) = \arctan[n_s(t) / (V_o a(t) + n_c(t))]$;

$n_c(t)$ and $n_s(t)$ are the in-phase and quadrature components of noise $n(t)$ respectively, each with zero mean and variance σ_n^2 . It is assumed that the IF filter is a finite band-pass integrator which is symmetric around f_{IF} with bandwidth $B_{IF} = 2/T$. With the demodulation time $\tau = T/2h$, $h \leq 1$ (narrowband CPFSK) and for the IF filter chosen, the correlation between $\theta_n(t)$ and $\theta_n(t-\tau)$ is zero. For other IF filter types such as Gaussian or second-order Butterworth, the noise correlation is negligibly small for $B_{IF} \geq 2$ and $h \leq 1$ (for NRZ) [36]. Further, the phase noise due to the receiver shot noise is statistically independent of that due to quantum phase noise. In the case of random NRZ data

$$I(t) = \sum_{k=-\infty}^{\infty} a_k p(t - kT) \quad (2.48)$$

where $a_k = \pm 1$ represents the k^{th} information bit and $p(t)$ is a rectangular pulse of unit amplitude and duration T seconds.

In a delay demodulation receiver the data decisions are based on the polarity of $V_{out}(t)$. Assuming a 'mark' is transmitted (say a_0) and under ideal CPFSK demodulation conditions viz. $2\pi f_{IF} \tau = (2n+1)\pi/2$, n is an integer and $2\pi \Delta f a_0 \tau = \pi/2$ for NRZ data, the phase of $V_{out}(t)$ at the sampling instant t_0 can be explicitly written as

$$\Delta\phi(t_0) = 2\pi f_{IF} \tau + \frac{\pi}{2} - \frac{\pi}{2} + \frac{\pi}{2} q(t_0) + \frac{\pi}{2} \sum_{k \neq 0} a_k q(t_0 - kT) + \Delta\alpha_n(t_0) + \Delta\theta_n(t_0) \quad \text{---(2.49)}$$

where $q(t) = \frac{1}{\tau} \int_{t-\tau}^t g(t_1) dt_1$

Note that the first two terms in (2.49) provide the expected phase change during the demodulation interval τ corresponding to the ideal situation, the next three terms, in fact, represent the undesired contribution to the phase due to GVD induced SPM and the last two terms represents the phase distortions due to quantum phase noise and the receiver noise respectively. Denoting the phase distortion of the signal only due to GVD induced SPM as :

$$\eta = \left[-\frac{\pi}{2} + \frac{\pi}{2} q(t_0) \right] + \frac{\pi}{2} \sum_{k \neq 0} a_k q(t_0 - kT) = \Delta\alpha_0 + \xi \quad (2.50)$$

and by virtue of the assumptions already made above for ideal CPFSK demodulation, it is possible to write the error probability expression conditioned on ξ as [39]

$$P(e|\xi) = P(-\pi \leq \Delta\phi(t) \bmod 2\pi \leq 0 | \xi) \quad (2.51a)$$

$$= \frac{1}{2} - \frac{1}{2} \rho e^{-\rho} \sum_n \frac{(-1)^n}{2n+1} \left[I_n\left(\frac{\rho}{2}\right) + I_{n+1}\left(\frac{\rho}{2}\right) \right]^2 \exp[-(2n+1)^2 \pi \Delta \nu \tau] \times \cos[(2n+1)(\Delta\alpha_0 + \xi)] \quad \text{---(2.51b)}$$

$$= \frac{1}{2} - F(\Delta\alpha_0, \xi) \quad (2.51c)$$

where $\rho = V_0^2 / 2\sigma_n^2$ is the IF SNR, $I_\alpha(x)$ is the modified Bessel function of first kind and order α , σ_n^2 is the variance of $n(t)$. The second term of implicitly defines $F(\Delta\alpha_0, \xi)$ in (2.51b). The average error probability can be evaluated as [41]

$$P(e) = \int_{-\infty}^{\infty} P(e|\xi) p_\xi(\xi) d\xi \quad (2.52)$$

Eqn. (2.52) can be evaluated by using the method of Gauss quadrature rule [41] .

Chapter-3

Results and Discussions

Following the theoretical analysis presented in chapter-2, the performance results for direct detection optical CPFSK system and heterodyne CPFSK system, are evaluated at a bit rate of 10 Gbit/s with different sets of receiver and system parameters. The parameters of the single-mode fibre used for numerical computations are : chromatic dispersion coefficient $D_c=15$ and -15 for wavelength $\lambda=1550\text{nm}$.

The bit error rate (BER) performance of direct detection CPFSK system is depicted in fig. 3.1 in presence of laser phase noise and receiver noise for $L=40$ km. The BER curve is plotted as a function of the received power, $P_s(\text{dBm})$ and the receiver sensitivity is defined as the optical power required to achieve a BER of 10^{-9} . In this figure, results are given for several values of input power when the modulation index $h=1.0$. In the same figure the reference curve has been shown for chromatic dispersion, $D_c=0.0$. The figure reveals that the BER decreases with increase in the input power. When the value of $D_c=0$, the receiver sensitivity is found to be -29.7 dBm. For a given BER (10^{-9}), to achieve more received power input power should be increased. From the plot it is observed that the BER performance decreases with the increase of received power, P_s .

For modulation index $h=0.5$ and length $L=40\text{km}$, the BER performance results are plotted in fig. 3.2 for $D_c=15$ ps/km-nm. Compared to fig. 3.1 it becomes evident that the performance degrades more sharply at higher value of h . The power penalty for $h=1.0$ is more compared to $h=0.5$. This is due to the fact that as h increases the difference between the 'mark' and 'space' frequencies in the CPFSK signal spectrum increases. As a consequence intersymbol interference caused by GVD & SPM increases at increased values of modulation index h .

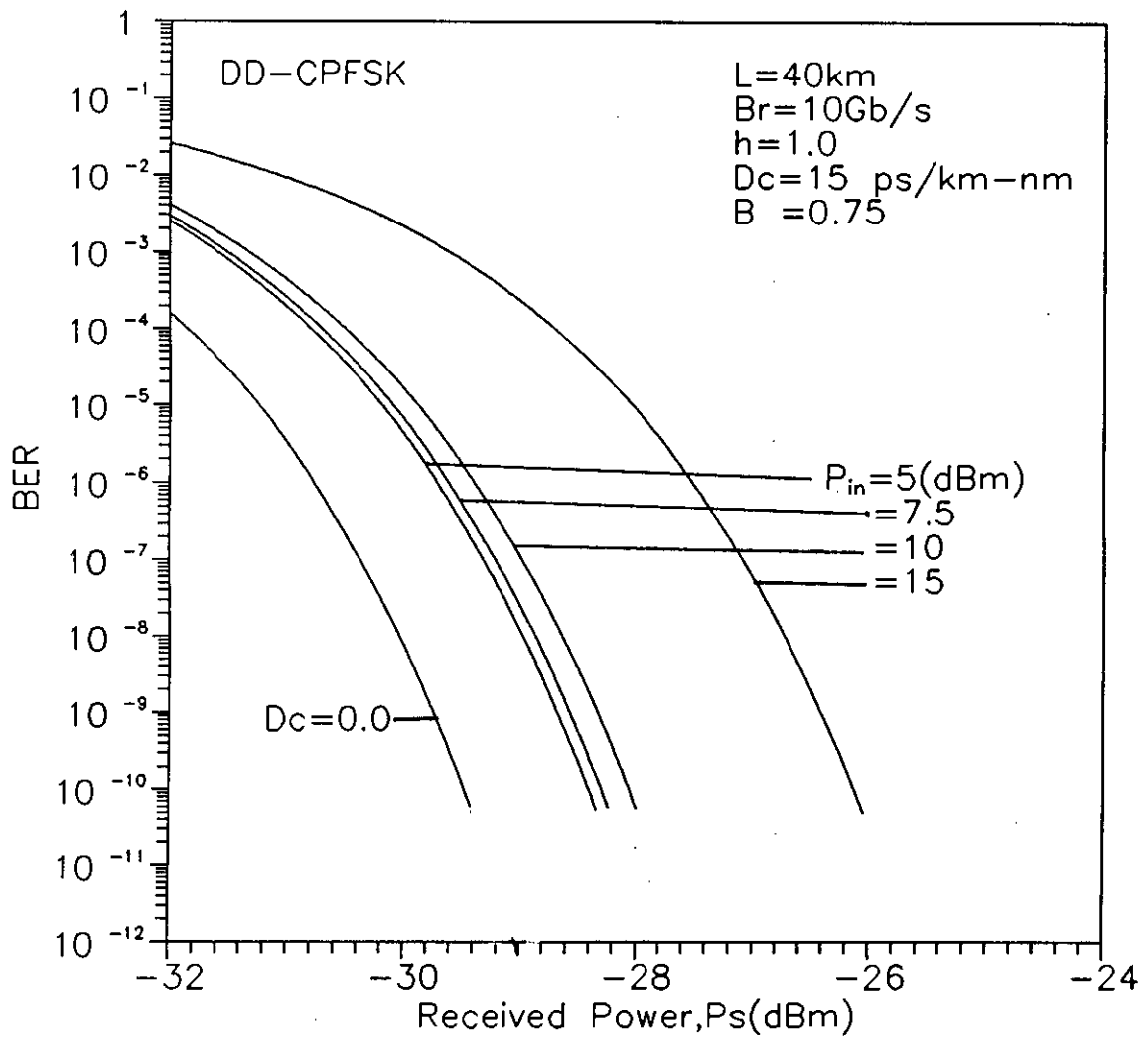


Fig.3.1 The bit error rate (BER) performance of direct detection optical CPFSK system at a bit rate 10 Gb/s with fibre chromatic dispersion $D_c=15$ ps/km-nm, band width $B=0.75$, fibre length $L=40$ km, wavelength of 1550 nm and modulation index $h=1.0$ for different values of received power P_s (dBm) at the receiver terminal.

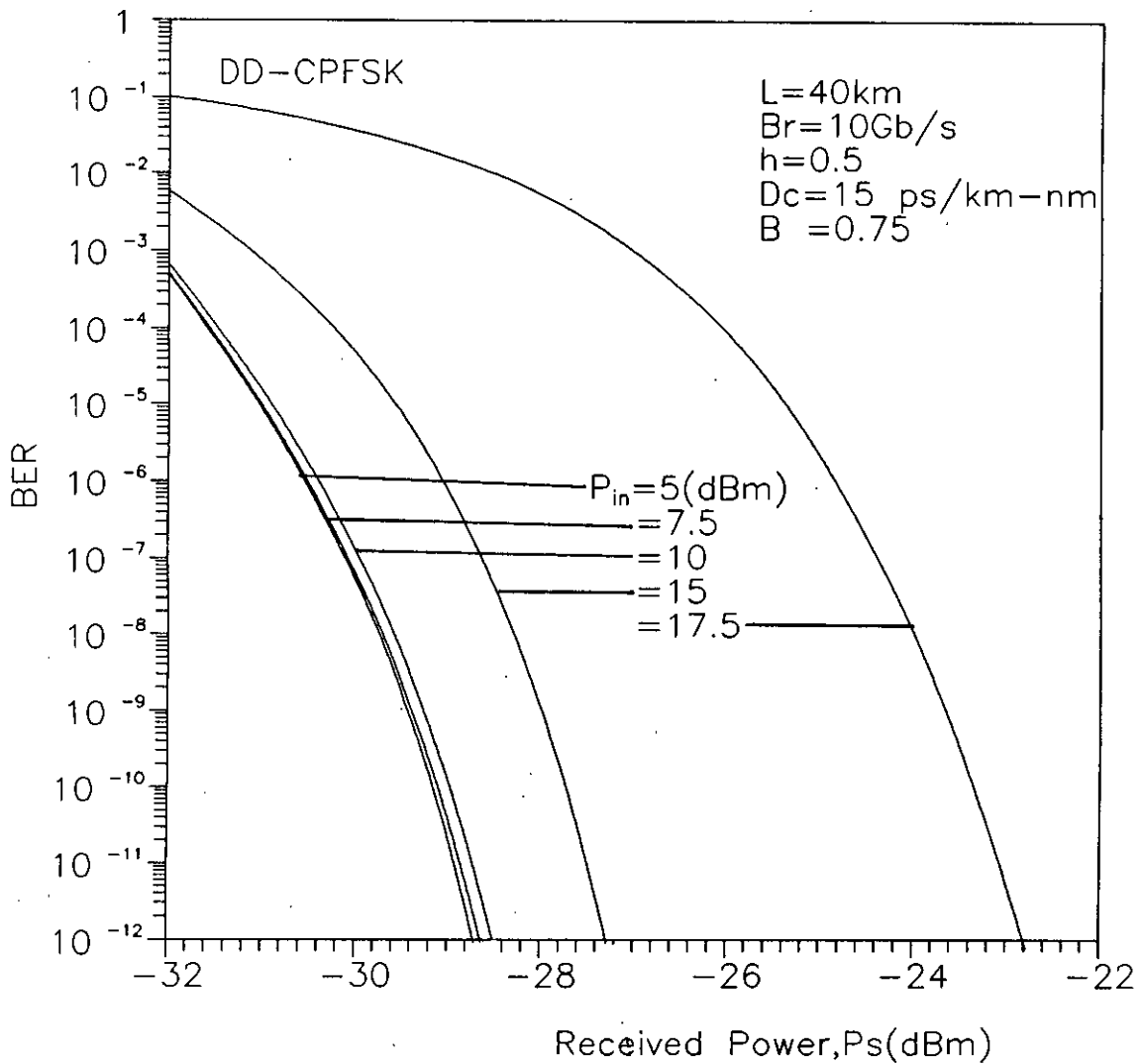


Fig.3.2 The bit error rate (BER) performance of direct detection optical CPFSK system at a bit rate 10 Gb/s with fibre chromatic dispersion $D_c=15$ ps/km-nm, band width $B=0.75$, fibre length $L=40$ km, wavelength of 1550 nm and modulation index $h=0.5$ for different values of received power P_s (dBm) at the receiver terminal.

In the presence of fibre chromatic dispersion and self-phase-modulation, the BER performance of CPFSK direct detection transmission system is shown in fig. 3.3 for fibre length $L=80\text{km}$ and modulation index $h=1.0$. Same figure has been plotted for $L=120\text{km}$ and $h=1.0$ in fig. 3.4. We notice that the performance of the system is more degraded due to the effect of fibre chromatic dispersion and self-phase modulation at longer fibre length.

When dispersion coefficient D_c is negative with fibre length $L=120\text{km}$, the results are shown in fig. 3.5. Compared to fig. 3.4 it is evident that negative dispersion factor causes the system performance improved at $\text{BER}=10^{-9}$.

The penalty in signal power suffered by the system due to the combined effect of Self-phase-modulation and fibre chromatic dispersion in direct detection CPFSK system, are determined from bit error rate (BER) curves at $\text{BER}=10^{-9}$. The plots of power penalty versus input power P_{in} (dBm) are shown in fig. 3.6 and 3.7 for modulation index $h=1.0$ and $h=0.5$ respectively. For both the cases four figures have been plotted for fibre span $L=40\text{ km}$, 60 km , 80 km and 120 km in the same graph with $D_c=15\text{ ps/km-nm}$. The figure depicts the variation of power penalty with input power and it is revealed that up to 7.5 dBm power penalty is almost constant and then increases almost linearly with increasing input power. Further the power penalty is found to be more for higher fibre length. For $h=0.5$ penalty increases abruptly after 12.5 dBm . Comparing fig. 3.6 and fig. 3.7 we note that power penalty is more for $h=1.0$ for same set of parameters. But for $h=0.5$ power penalty increases abruptly compared to $h=1$ shown in fig. 3.6. It is also revealed that the allowable input power for a given power penalty is higher for $h=0.5$ compared to $h=1$.

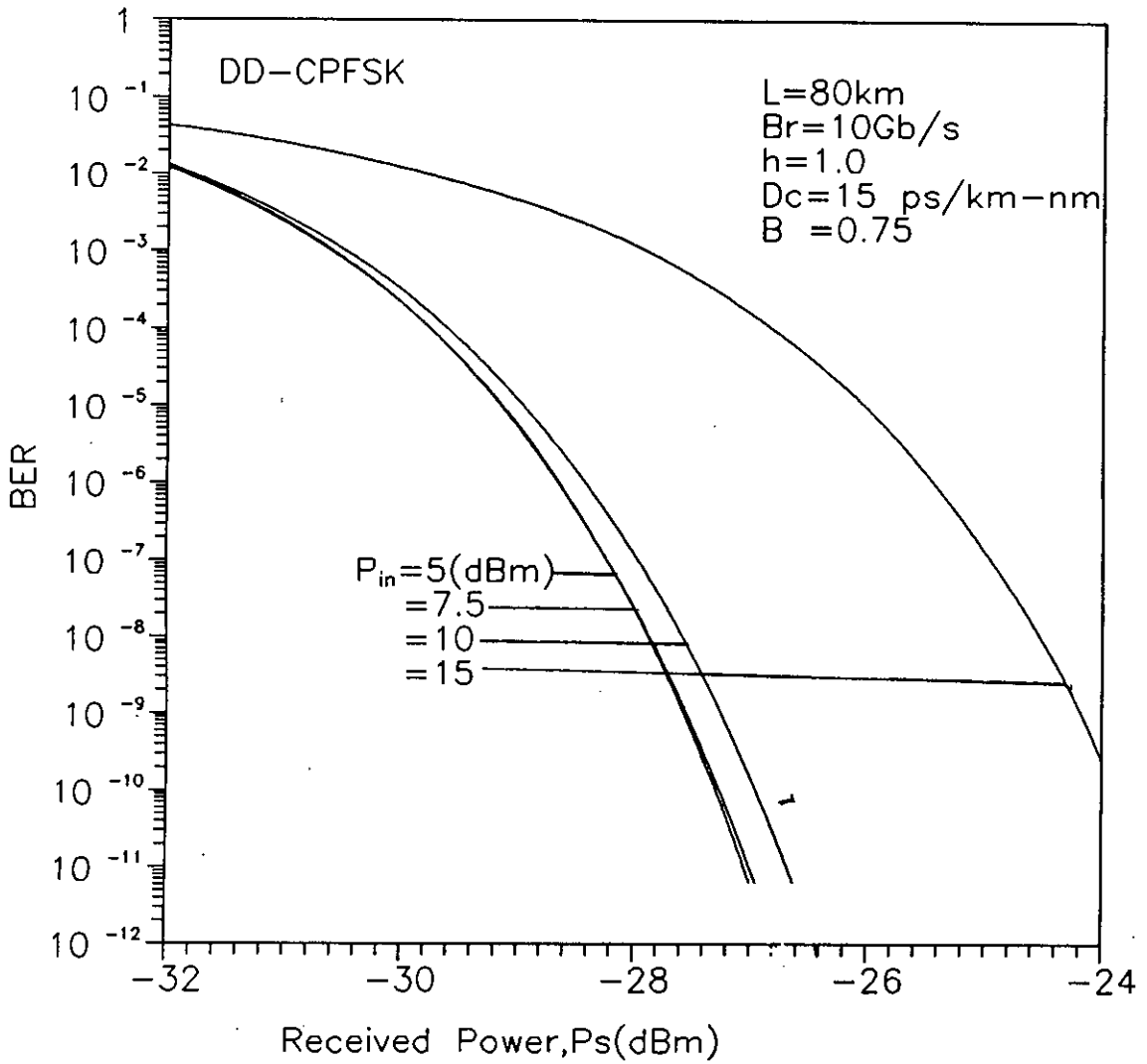


Fig.3.3 The bit error rate (BER) performance of direct detection optical CPFSK system at a bit rate 10 Gb/s with fibre chromatic dispersion $D_c=15$ ps/km-nm, band width $B=0.75$, fibre length $L=80$ km, wavelength of 1550 nm and modulation index $h=1.0$ for different values of received power P_s (dBm) at the receiver terminal.

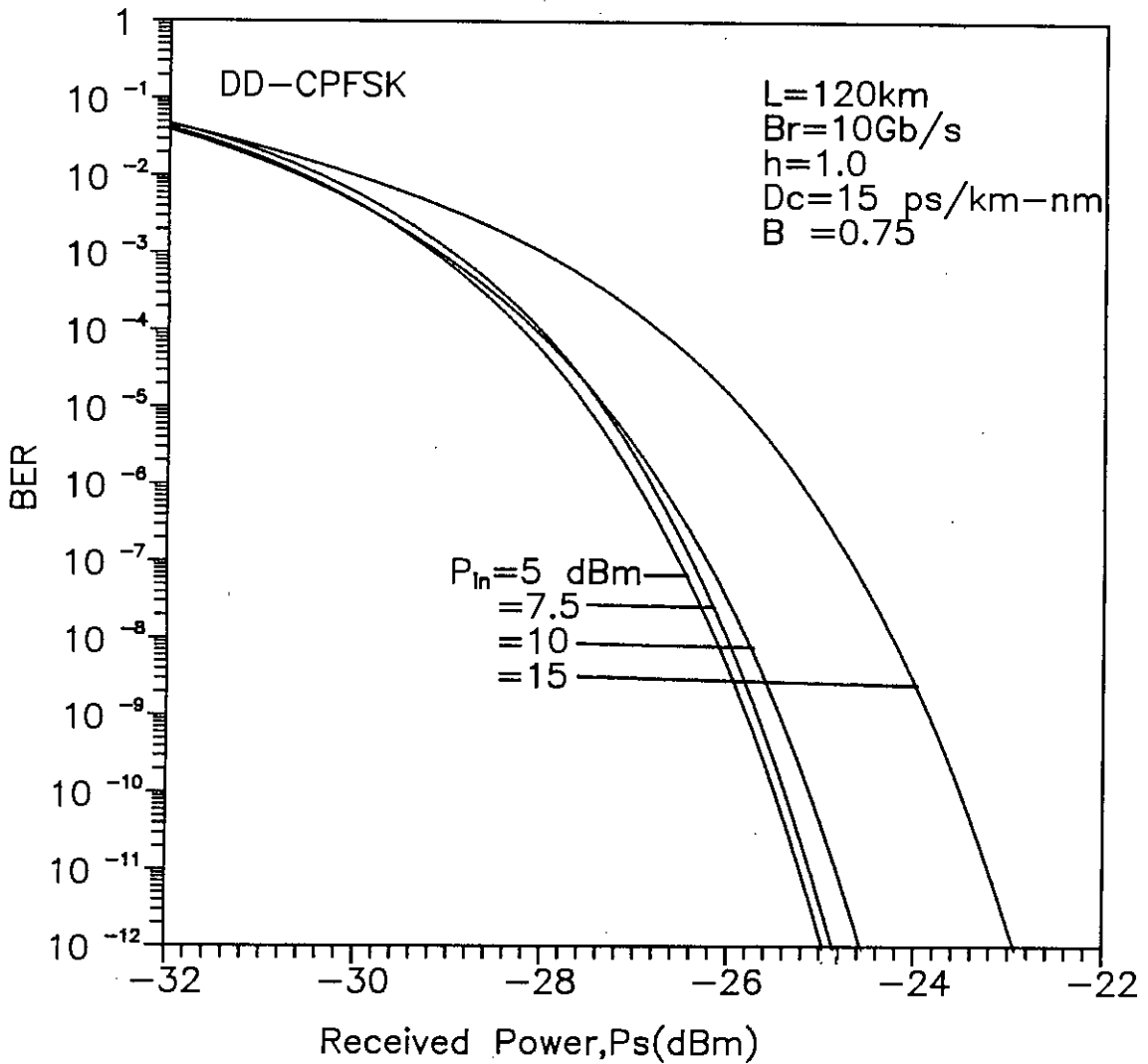


Fig.3.4 The bit error rate (BER) performance of direct detection optical CPFSK system at a bit rate 10 Gb/s with fibre chromatic dispersion $D_c=15\text{ ps/km-nm}$, band width $B=0.75$, fibre length $L=120\text{ km}$, wavelength of 1550 nm and modulation index $h=1.0$ for different values of received power P_s (dBm) at the receiver terminal.

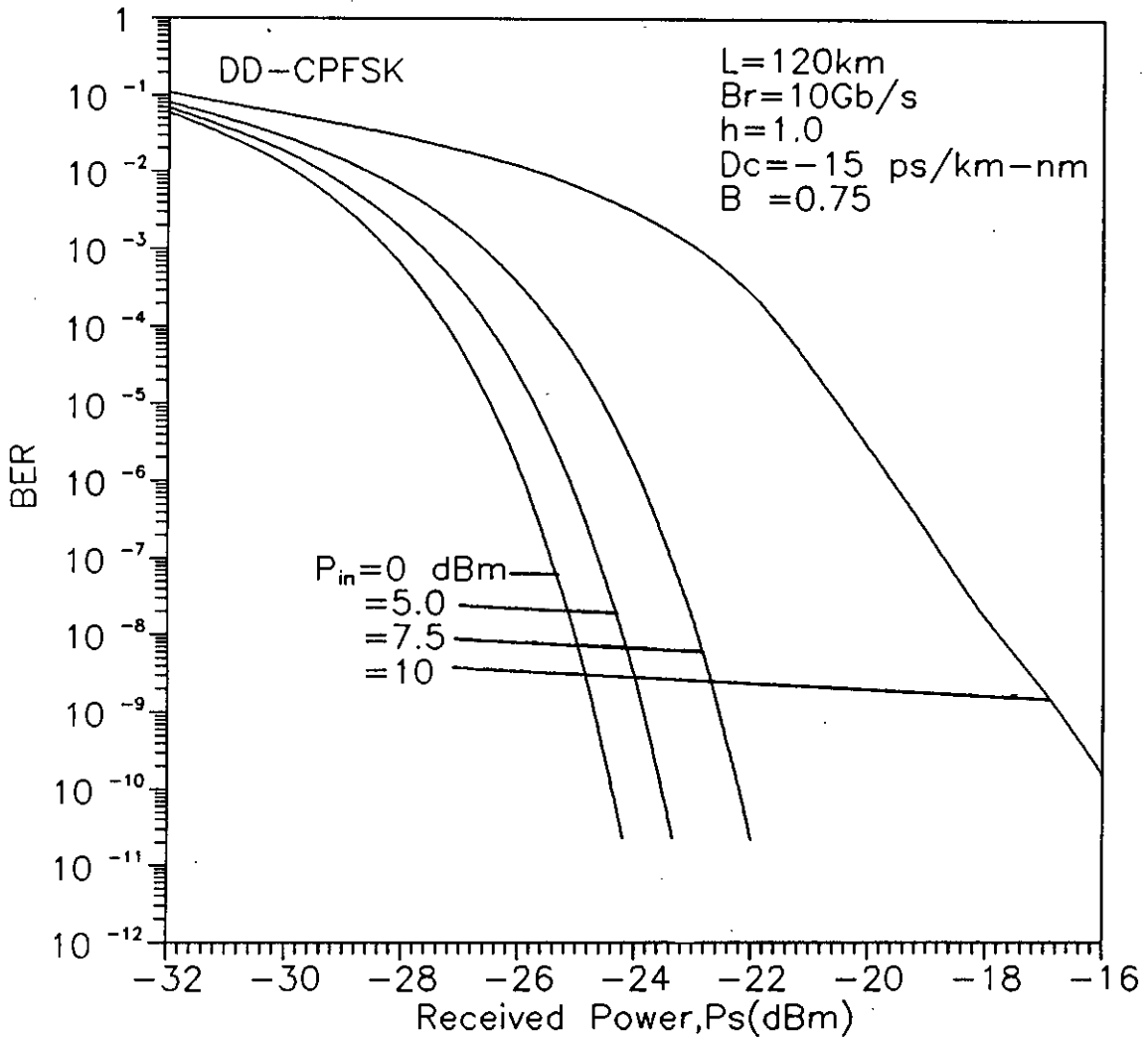


Fig.3.5 The bit error rate (BER) performance of direct detection optical CPFSK system at a bit rate 10 Gb/s with fibre chromatic dispersion $D_c=-15$ ps/km-nm, band width $B=0.75$, fibre length $L=120$ km, wavelength of 1550 nm and modulation index $h=1.0$ for different values of received power P_s (dBm) at the receiver terminal.

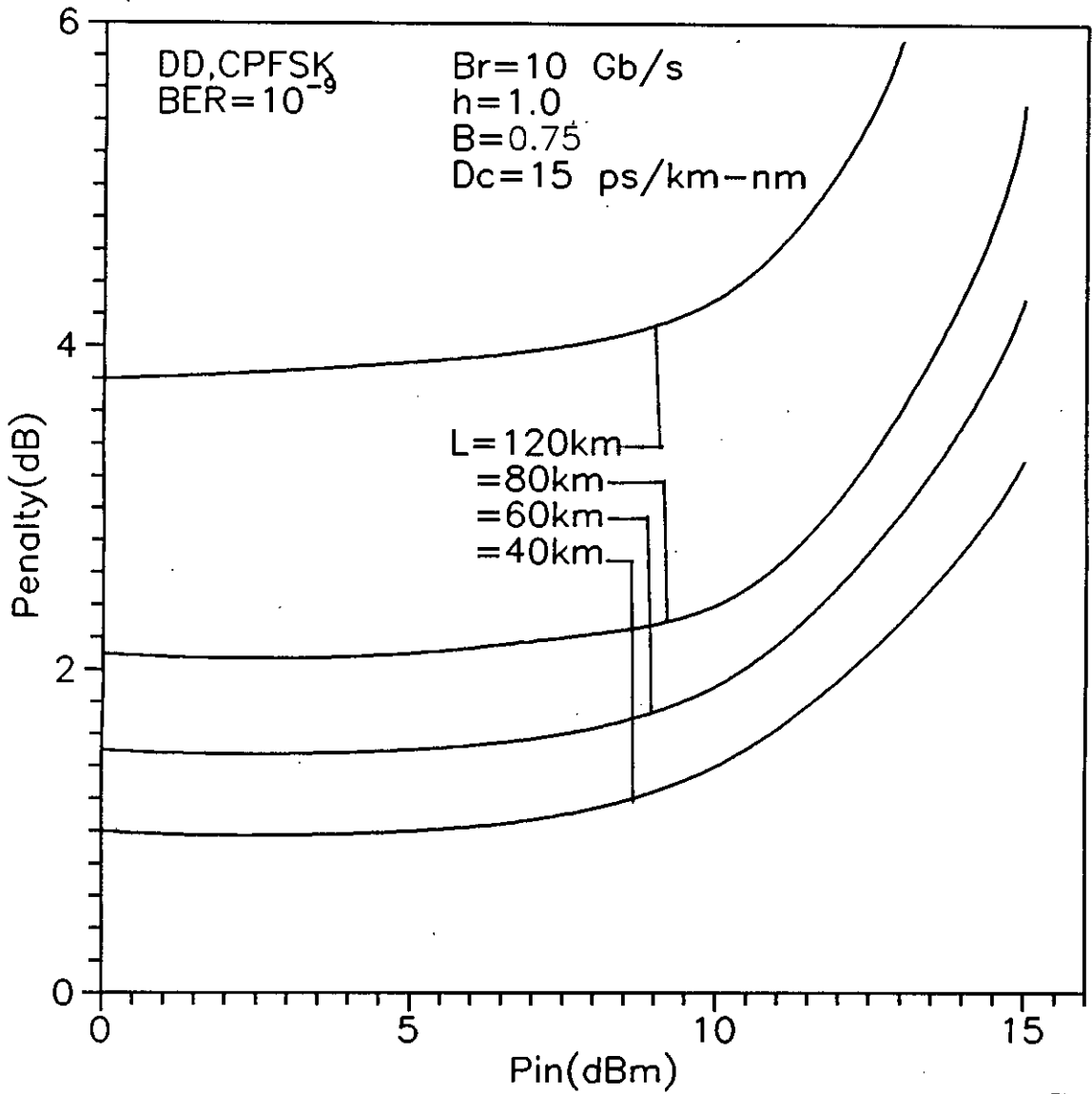


Fig.3.6 Plots of penalty in signal power due to Self-phase-modulation & fibre chromatic dispersion at $BER=10^{-9}$ versus power input with bit rate $Br=10$ Gb/s, dispersion co-efficient $Dc=15$ ps/km-nm, band width $B=0.75$ and modulation index $h=1.0$ for different lengths $L=40$ km, 60 km, 80 km, 120 km at a Direct detection CPFSK receiver.

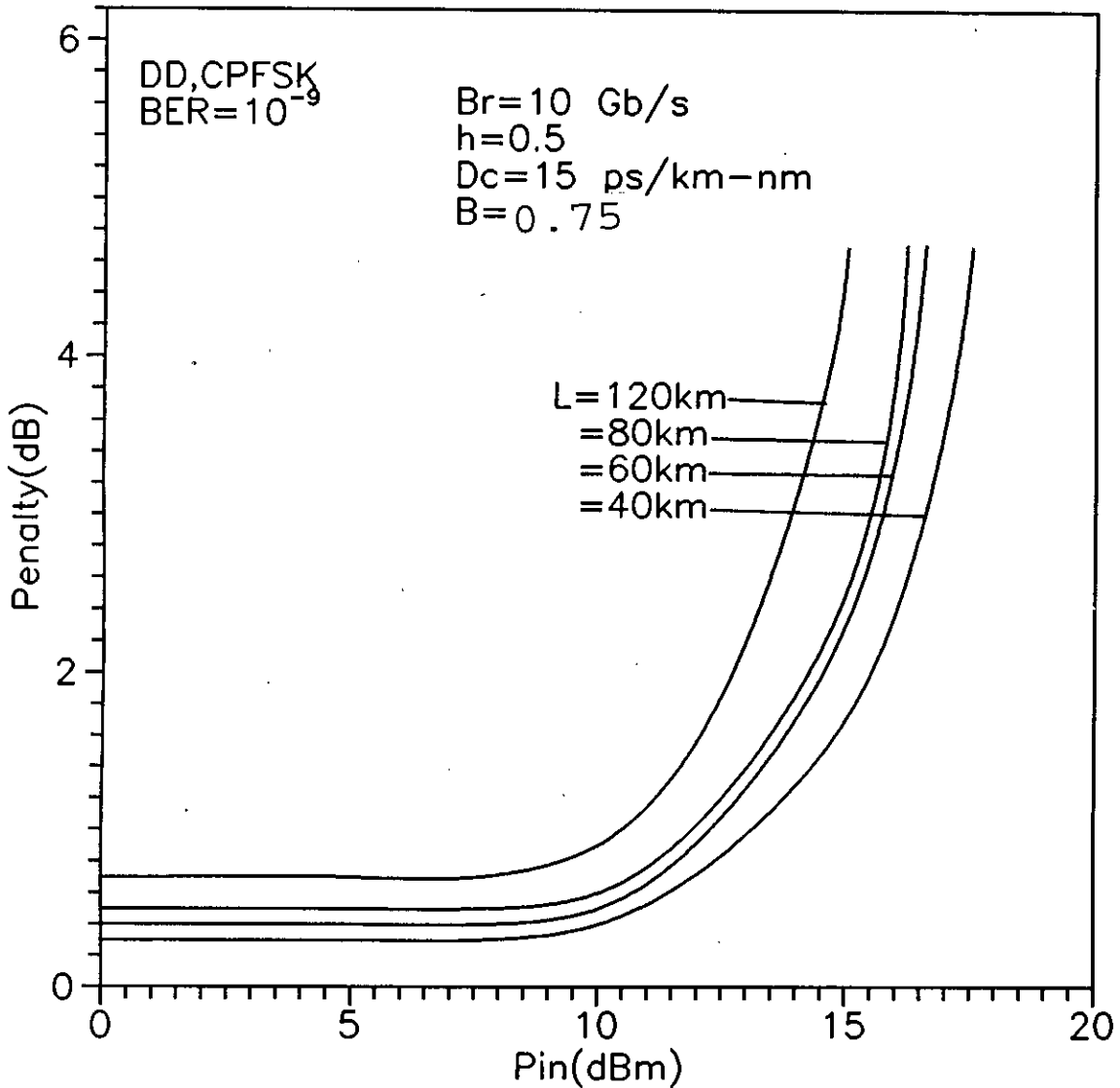


Fig.3.7 Plots of penalty in signal power due to Self-phase-modulation & fibre chromatic dispersion at BER= 10^{-9} versus power input with bit rate Br=10 Gb/s, dispersion coefficient Dc=15 ps/km-nm, band width B=0.75 and modulation index h=0.5 for different lengths L=40km, 60km, 80km, 120km at a Direct detection CPFSK receiver.

Similar plots of penalty versus input power are also shown in fig. 3.8 and 3.9 for negative dispersion coefficient $D_c = -15$ ps/km-nm. Fig. 3.8 and 3.9 have been drawn for $h = 1.0$ and $h = 0.5$ respectively. For negative D_c , variation of power penalty is less compared to positive dispersion.

As seen from the figures that penalty remains almost constant up to 12.5 dBm when $D_c = -15$ where it is up to 7.5 dBm for $D_c = 15$ for $L = 40$ km. This negative dispersion allows more input power for a given power penalty. This is due to the fact that for negative dispersion, the effect of SPM is opposite to that of GVD. As a consequence, the penalty remains constant up to higher value of input power. Further increase in input power causes the effect of SPM to be increased more.

When the modulation index h is increased from 0.6 to 0.8, the receiver performance results are given in fig. 3.10 for length $L = 40$ km and chromatic dispersion coefficient $D_c = 15$. The effect of increased modulation index on the system performance is noticed when these curves are compared to fig. 3.1 to 3.5. It becomes clear that the BER increases with increase in the value of modulation index h for a given value of received power. As a consequence the system suffers more penalty in signal power at increased modulation index. This is due to broadened spectrum at higher modulation index and the effect of dispersion is more prominent at increased bandwidth of the signal spectrum.

The variation of power penalty with modulation index h is plotted in fig. 3.11 and fig. 3.12 for direct detection CPFSK at fibre length $L = 40$ km and 80 km respectively. It is observed that penalty increases almost linearly with increasing value of modulation index. However, as mentioned before, the penalty is found to be higher at higher values of modulation index. For different values of input power three different curves have been plotted in same plot. When input power is 15 dBm penalty versus modulation index curve (fig. 3.11) shows nonlinear characteristics.

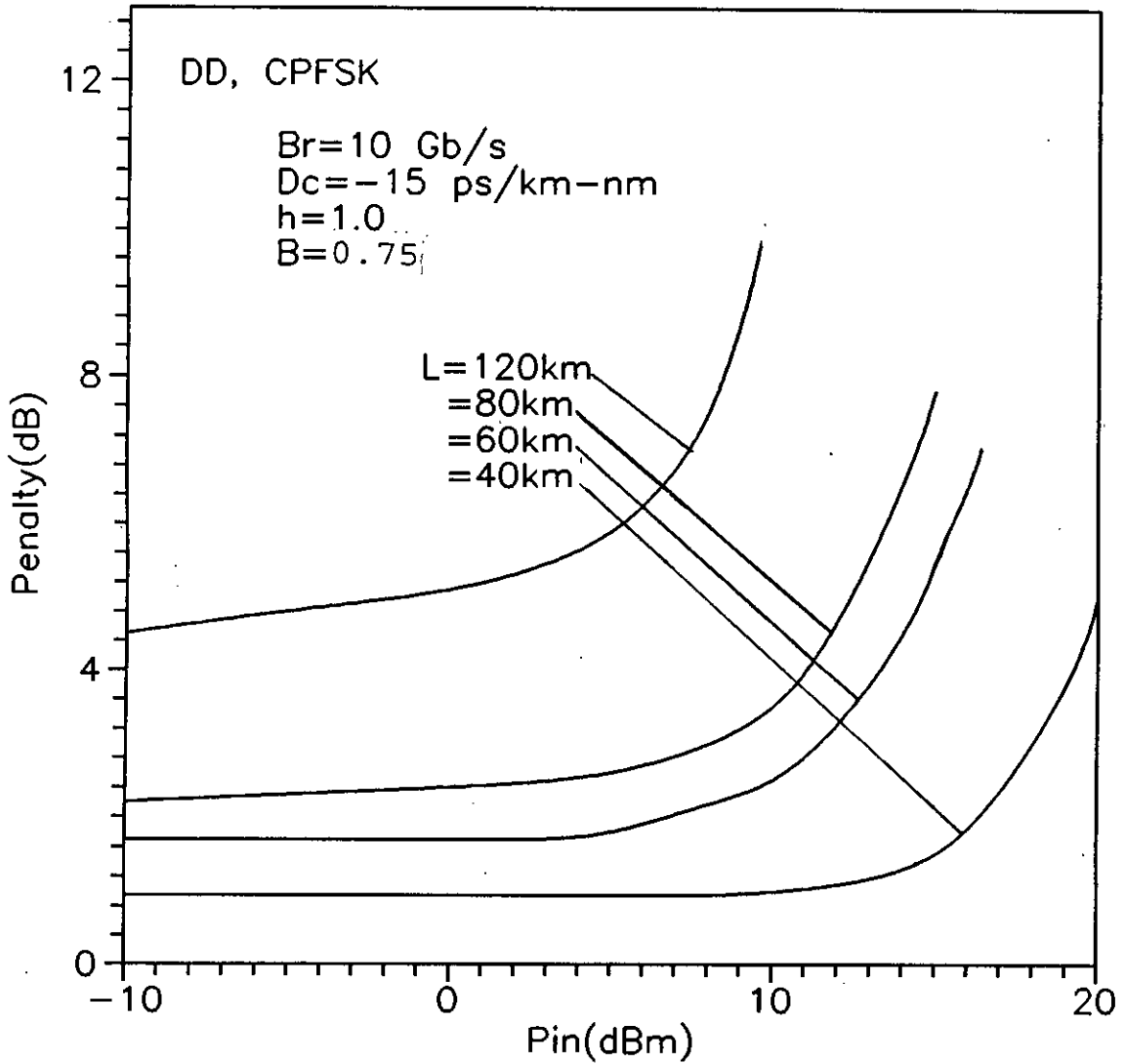


Fig.3.8 Plots of penalty in signal power due to Self-phase-modulation & fibre chromatic dispersion at BER= 10^{-9} versus power input with bit rate Br=10 Gb/s, dispersion coefficient Dc=-15 ps/km-nm, band width B=0.75 and modulation index h=1.0 for different lengths L=40km, 60km, 80km, 120km at a direct detection CPFSK receiver.

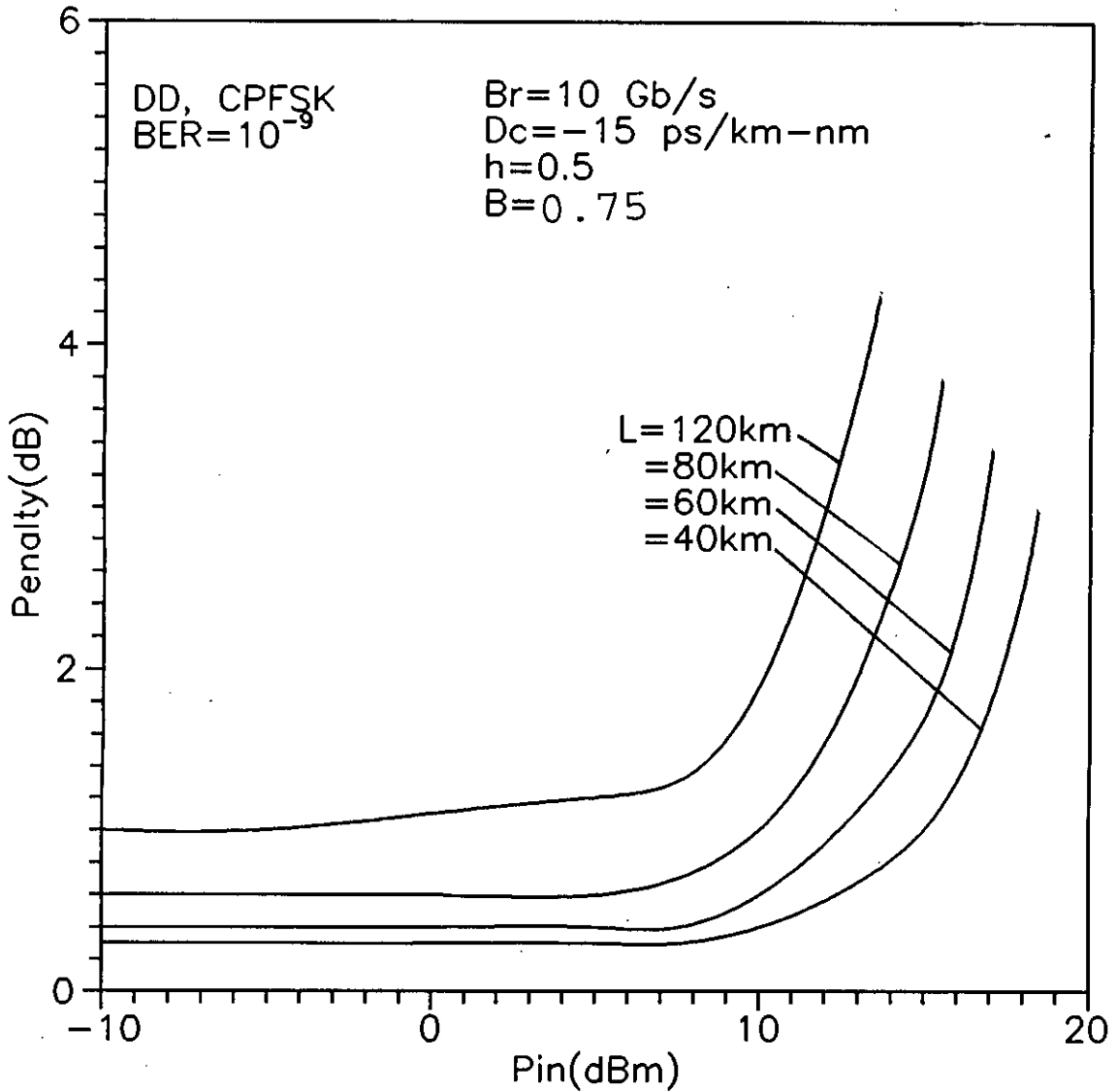


Fig.3.9 Plots of penalty in signal power due to Self-phase-modulation & fibre chromatic dispersion at BER=10⁻⁹ versus power input with bit rate Br=10 Gb/s, dispersion coefficient Dc=-15 ps/km-nm, band width B=0.75 and modulation index h=0.5 for different lengths L=40km, 60km, 80km, 120km at a direct detection CPFSK receiver.

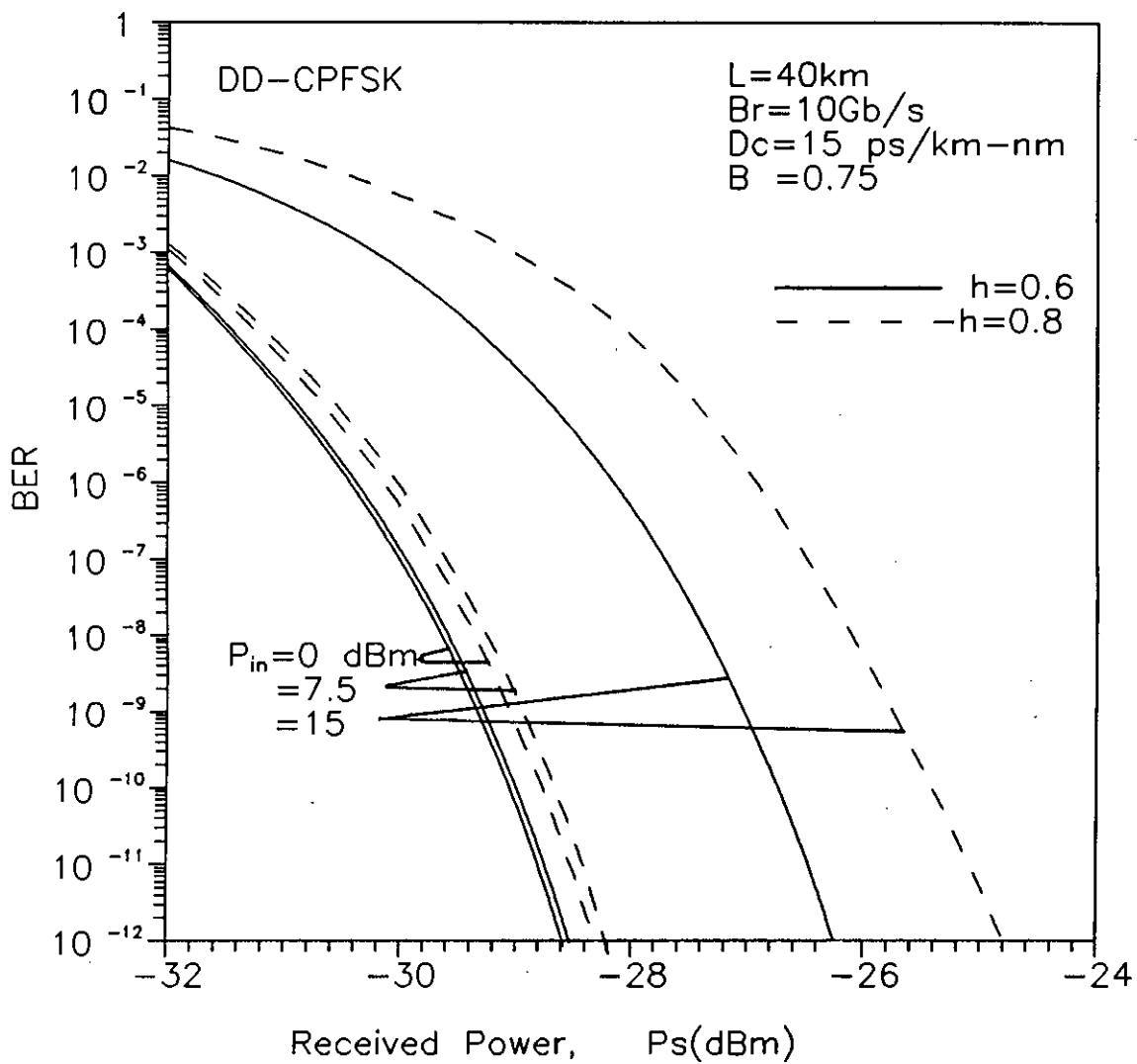


Fig3.10 Variation of the bit error rate (BER) performance due to different values of modulation index (say, $h=0.6, 0.8$) of a direct detection CPFSK receiver at a bit rate 10 Gb/s with fibre chromatic dispersion $D_c=15\text{ ps/km-nm}$, fibre length $L=40\text{km}$, band width $B=0.75$, for several values of received power P_s .

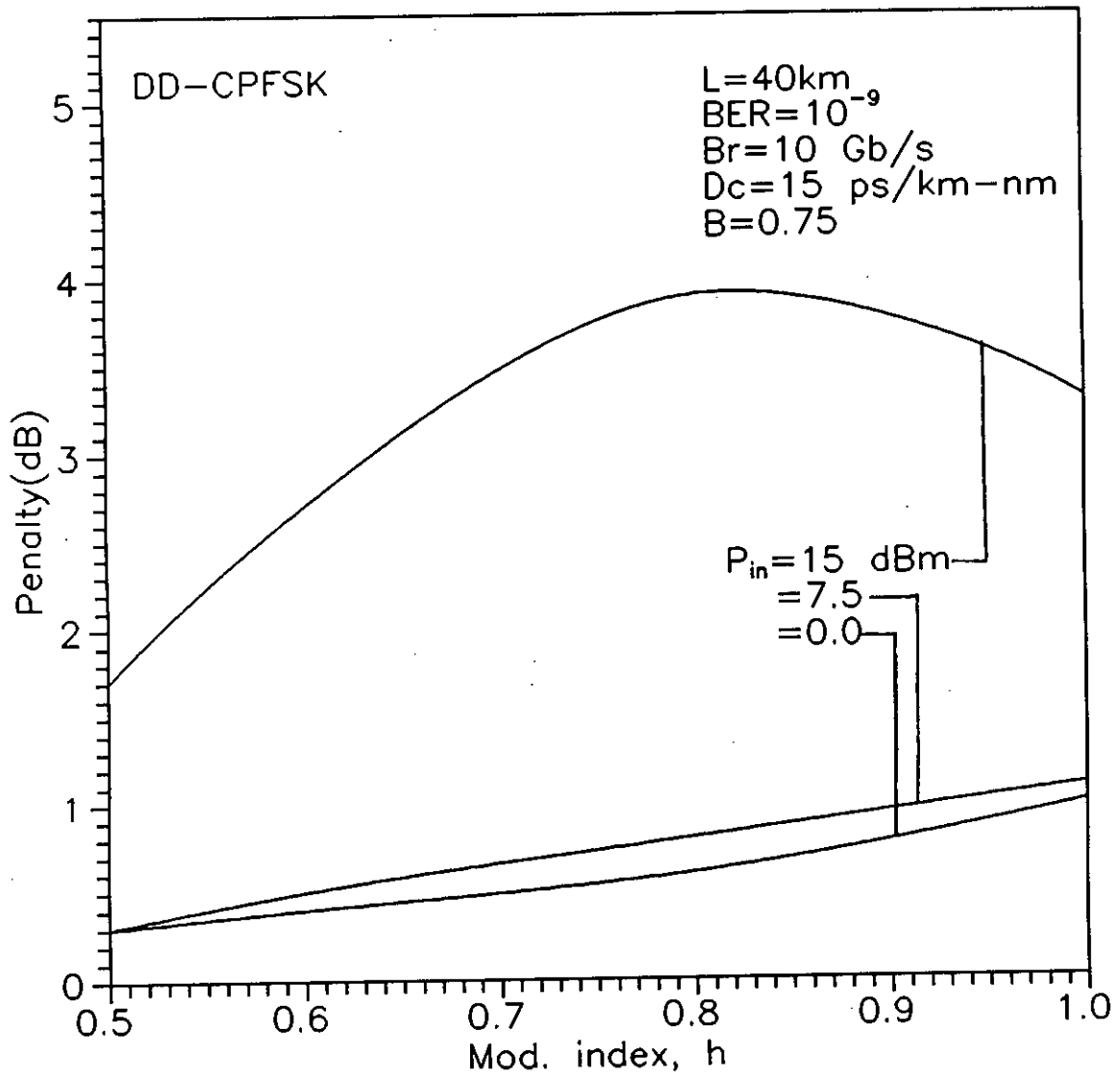


Fig.3.11 Variation of power penalty in signal power due to combined effect of Self-phase-modulation & fibre chromatic dispersion at $\text{BER}=10^{-9}$ versus modulation index (h) with fibre length $L=40\text{km}$, $B_r=10\text{ Gb/s}$, dispersion coefficient $D_c=15$ and band width $B_{IF}=2$ for different values of input power $P_{in}=-10, 0, 15\text{ dB}$ for a direct detection CPFSK receiver.

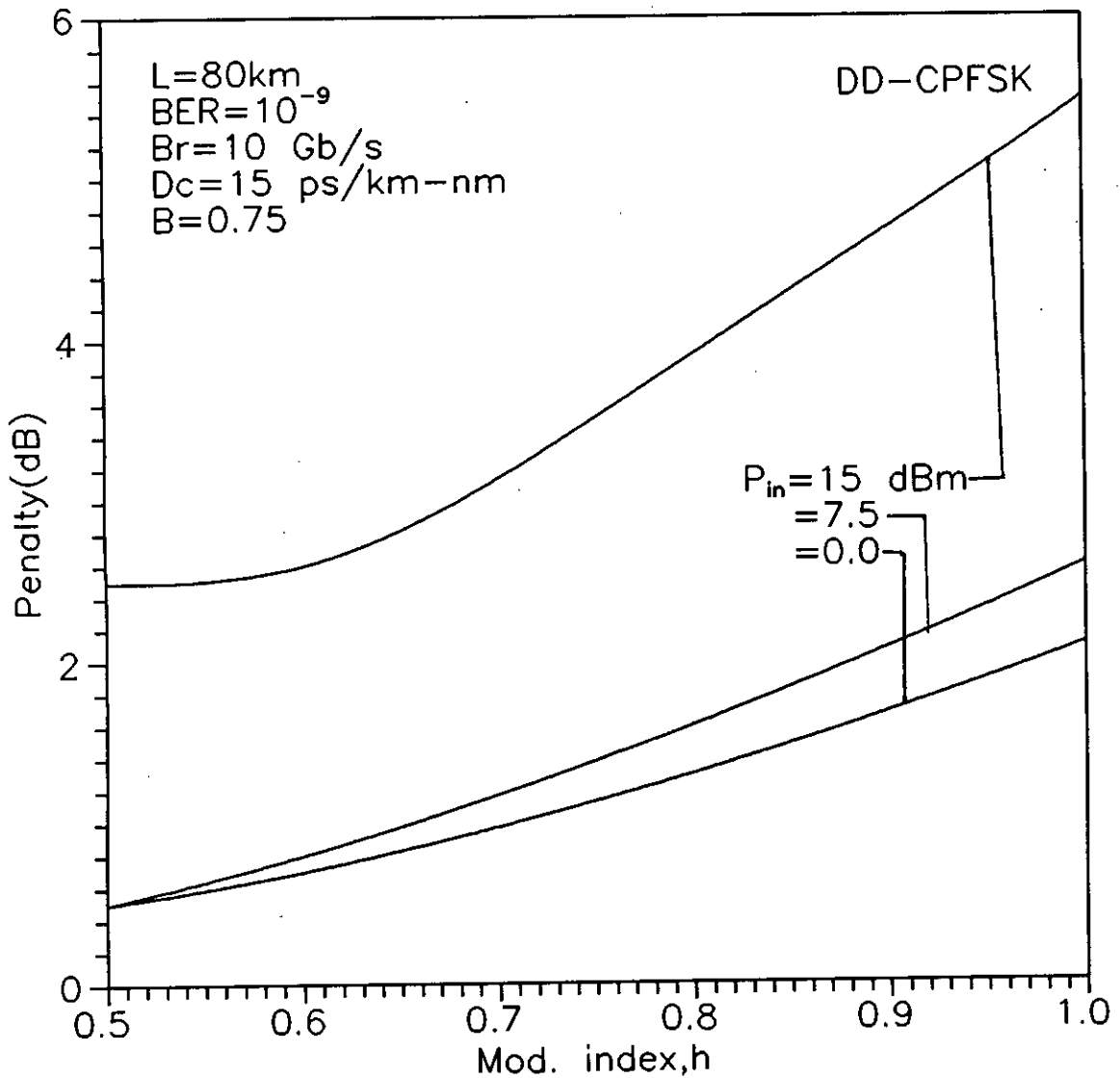


Fig.3.12 Variation of power penalty in signal power due to combined effect of Self-phase-modulation & fibre chromatic dispersion at $\text{BER}=10^{-9}$ versus modulation index (h) with fibre length $L=40\text{km}$, $B_r=10\text{ Gb/s}$, dispersion coefficient $D_c=15$ and band width $B_{IF}=2$ for different values of input power $P_{in}=15, 7.5, 0.0\text{ dBm}$ for a direct detection CPFSK receiver.

In this case penalty increases with higher slope up to $h=0.8$ and then degrades slowly. But in case of greater fibre length ($L=80$ km) the penalty increases almost linearly with modulation index for different input power (fig. 3.12).

In fig. 3.13 the BER performance has been shown for heterodyne CPFSK receiver. For specified length $L=40$ km at modulation index $h=1.0$ and dispersion coefficient $D_c=-15$ ps/km-nm BER performance curves have been plotted for different values of input power. At the same plot, the reference curve for $D_c=0$ has been shown. Received power at $BER=10^{-9}$ for heterodyne CPFSK receiver is found -45 dBm. Similar curves have been plotted in fig. 3.14 for $h=0.5$. From comparison with the previous curve it is observed that BER performance improves for lower modulation index as in the case of direct detection.

In fig. 3.15 BER performance curve has been plotted for length $L=80$ km and $D_c=-15$ ps/km-nm. With the increased fibre length BER performance increases. For same length and same modulation index fig. 3.16 has been plotted at dispersion $D_c=+15$ ps/km-nm. Fig. 3.17 has been plotted for length $L=120$ km and setting all parameters as before but changing D_c as negative. For higher length BER is more at certain received power.

Power penalty versus input power curves have been plotted for heterodyne CPFSK receiver for different fibre length viz. $L=120$ km, 80 km, 60 km and 40 km in figure 3.18 and fig. 3.19 for $h=1.0$ and $h=0.5$ respectively at $D_c=-15$ ps/km-nm. Penalty is constant up to input power $P_{in}=7.5$ dBm in both case. Comparing to fig. 3.18 and fig. 3.19 it is observed that penalty is slightly higher for $h=1.0$ than $h=0.5$. Again, comparing to fig. 3.6 to fig. 3.9 for $h=1.0$, it is found that penalty curve increases after 7.5 dBm in fig. 3.6 but in fig. 3.18 penalty slightly decreases at 7.5 dBm and then increases again. Penalty is more in heterodyne CPFSK system than direct detection CPFSK system for specified fibre length. Same variation we also observed in fig. 3.7 and fig. 3.19 for $h=0.5$. But for heterodyne CPFSK system

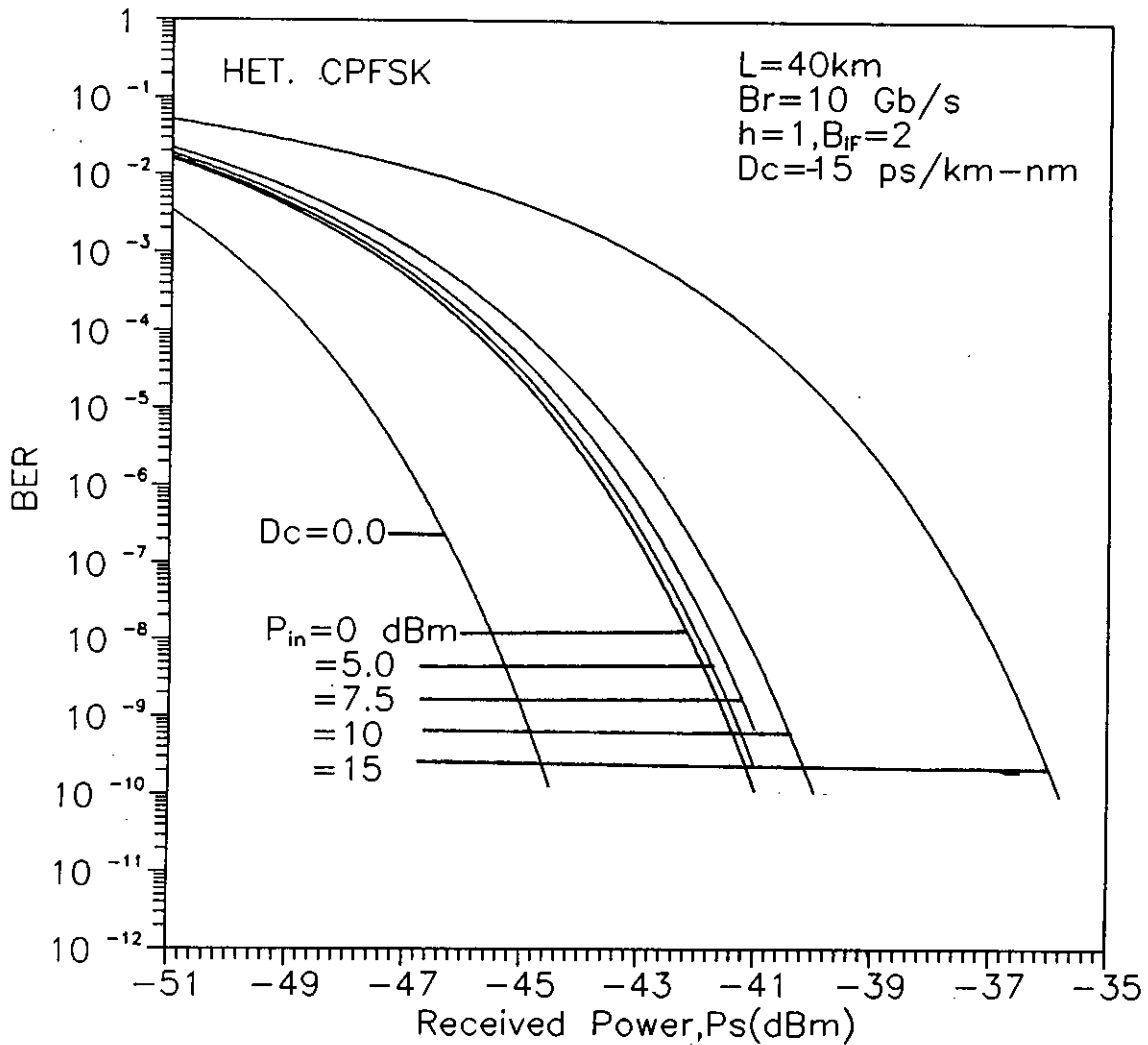


Fig.3.13 The bit error rate (BER) performance of a heterodyne optical CPFSK system at a bit rate 10 Gb/s with fibre chromatic dispersion $D_c=-15$ ps/km-nm, band width $B_{IF}=2$, fibre length $L=40$ km, wavelength of 1550 nm and modulation index $h=1.0$ for different values of received power P_s (dBm) at the receiver terminal.

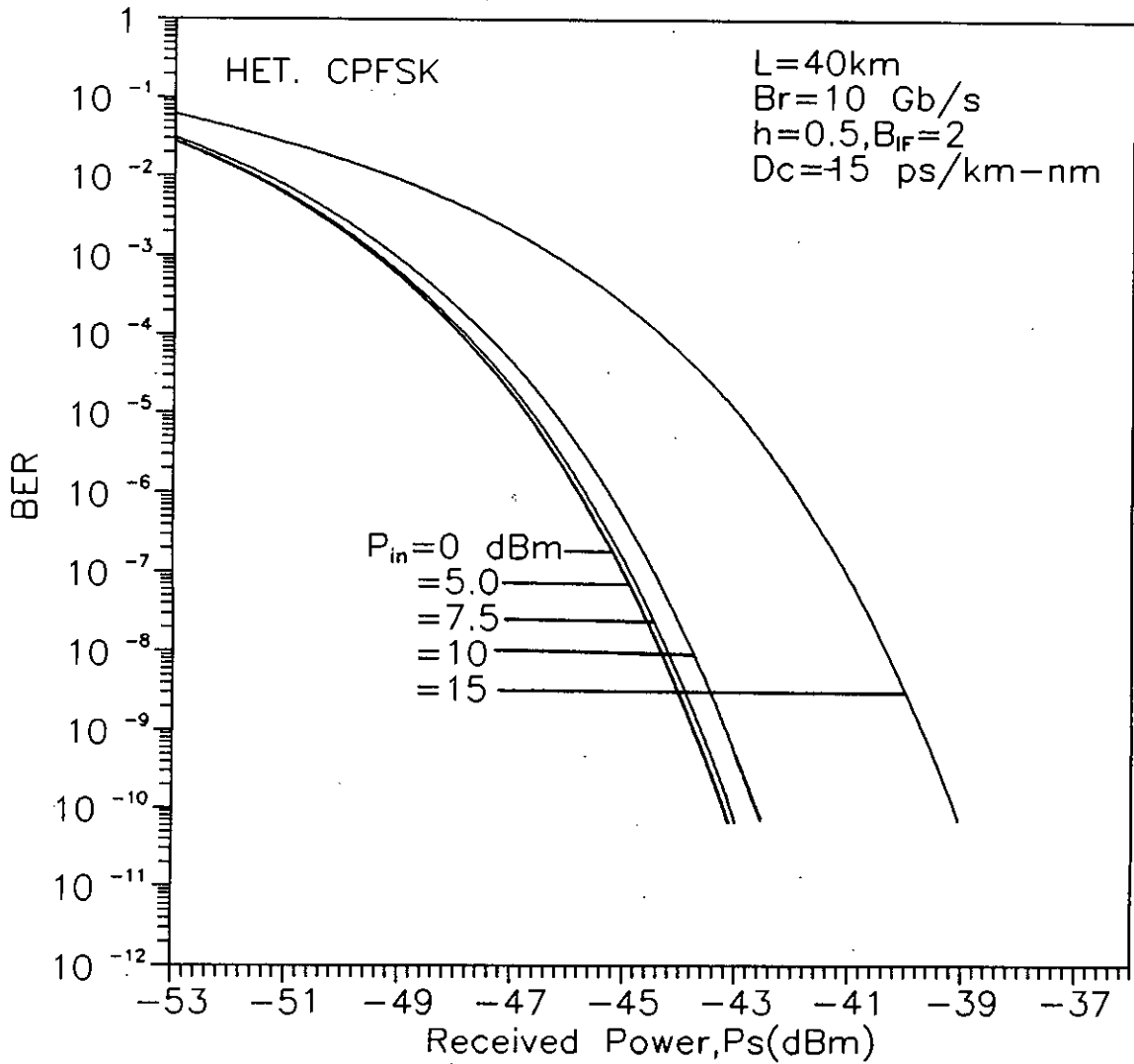


Fig.3.14 The bit error rate (BER) performance of a heterodyne optical CPFSK system at a bit rate 10 Gb/s with fibre chromatic dispersion $D_c=-15\text{ ps/km-nm}$, bandwidth $B_{IF}=2$, fibre length $L=40\text{ km}$, wavelength of 1550 nm and modulation index $h=0.5$ for different values of received power P_s (dBm) at the receiver terminal.

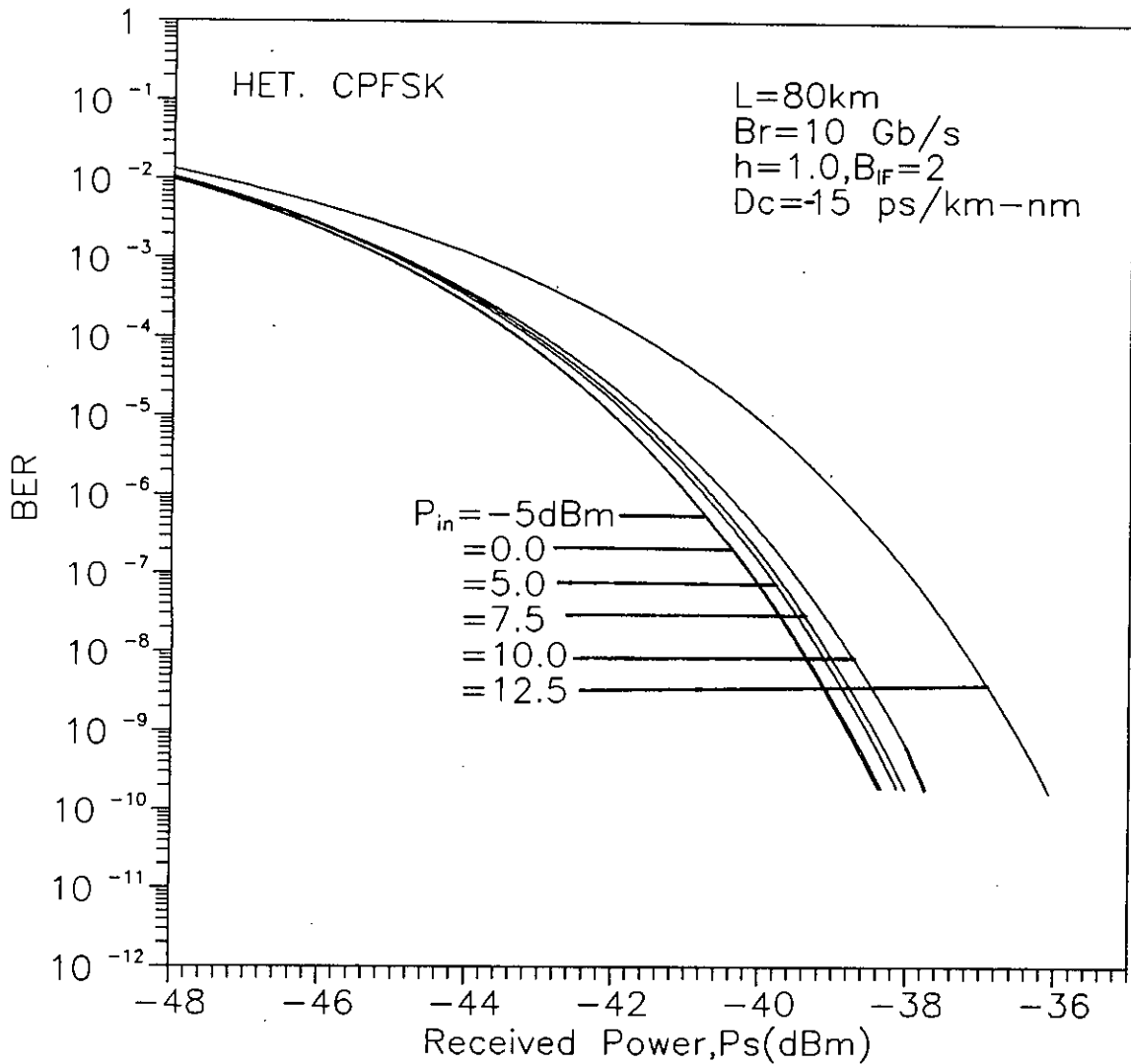


Fig.3.15 The bit error rate (BER) performance of a heterodyne optical CPFSK system at a bit rate 10 Gb/s with fibre chromatic dispersion $D_c=-15\text{ ps/km-nm}$, bandwidth $B_{IF}=2$, fibre length $L=80\text{ km}$, wavelength of 1550 nm and modulation index $h=1.0$ for different values of received power P_s (dBm) at the receiver terminal.

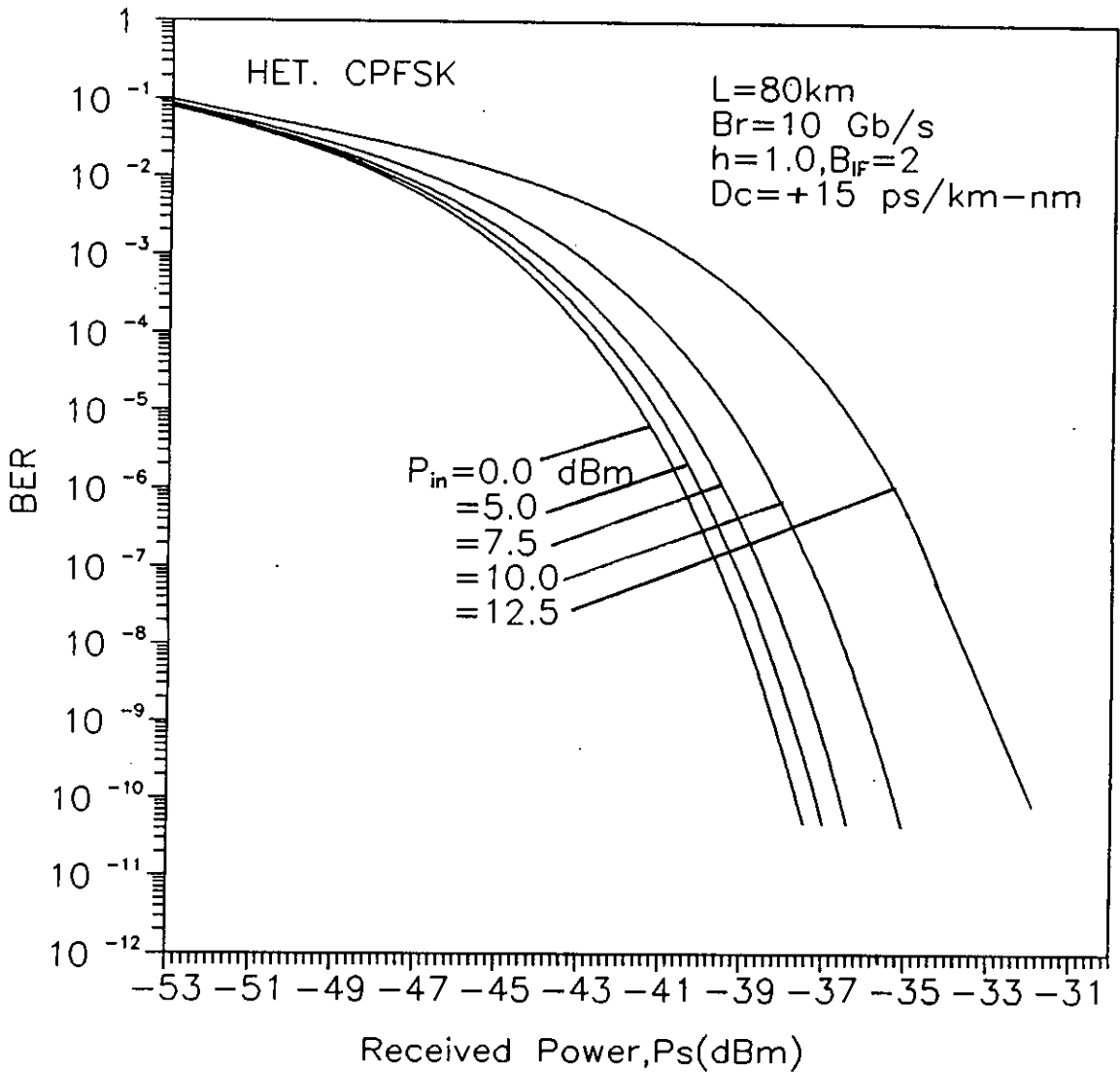


Fig.3.16 The bit error rate (BER) performance of a heterodyne optical CPFSK system at a bit rate 10 Gb/s with fibre chromatic dispersion $D_c=+15\text{ ps/km-nm}$, band width $B_{IF}=2$, fibre length $L=80\text{ km}$, wavelength of 1550 nm and modulation index $h=1.0$ for different values of received power P_s (dBm) at the receiver terminal.

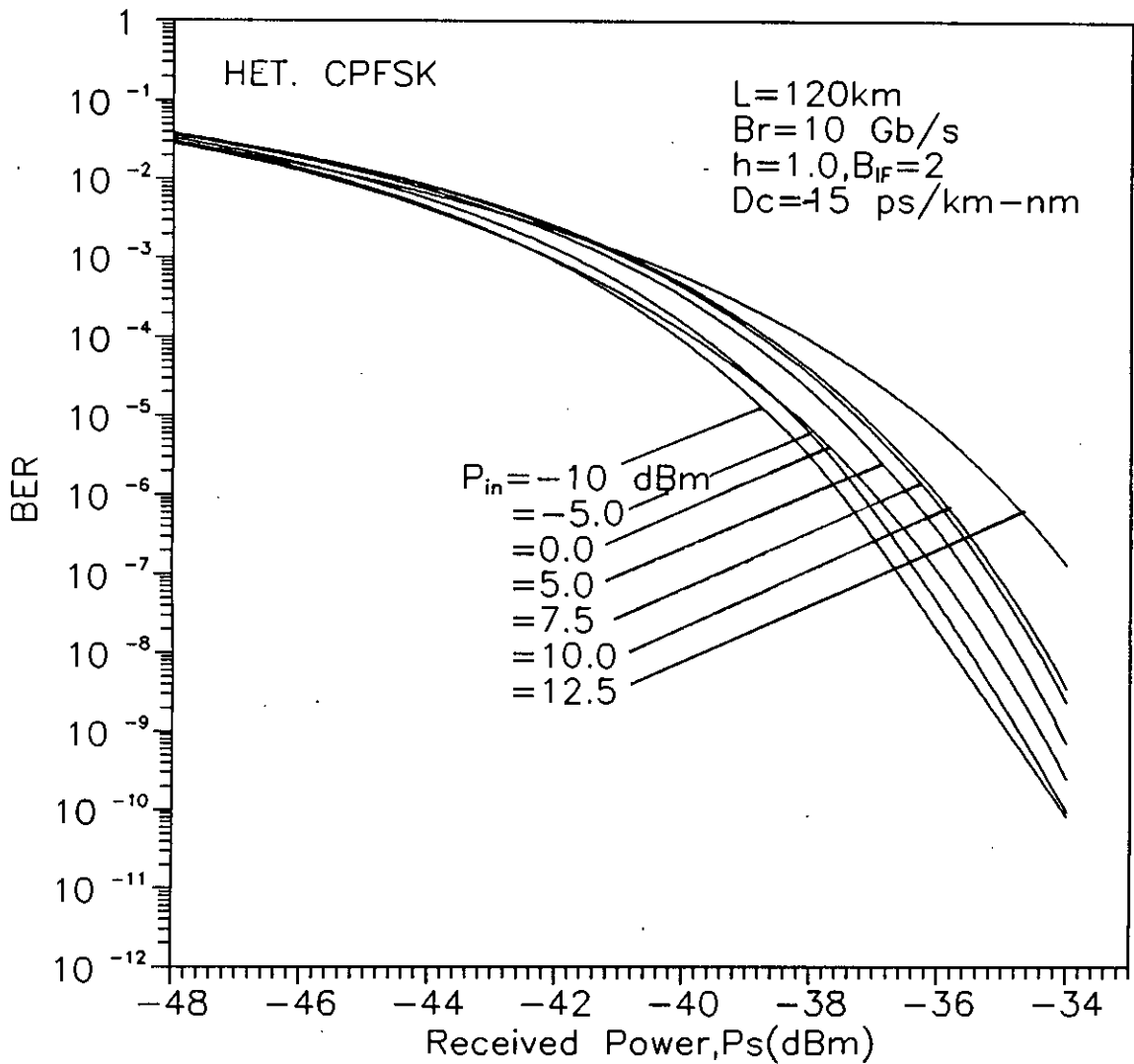


Fig.3.17 The bit error rate (BER) performance of a heterodyne optical CPFSK system at a bit rate 10 Gb/s with fibre chromatic dispersion $D_c=15\text{ ps/km-nm}$, bandwidth $B_{IF}=2$, fibre length $L=120\text{ km}$, wavelength of 1550 nm and modulation index $h=1.0$ for different values of received power P_s (dBm) at the receiver terminal.

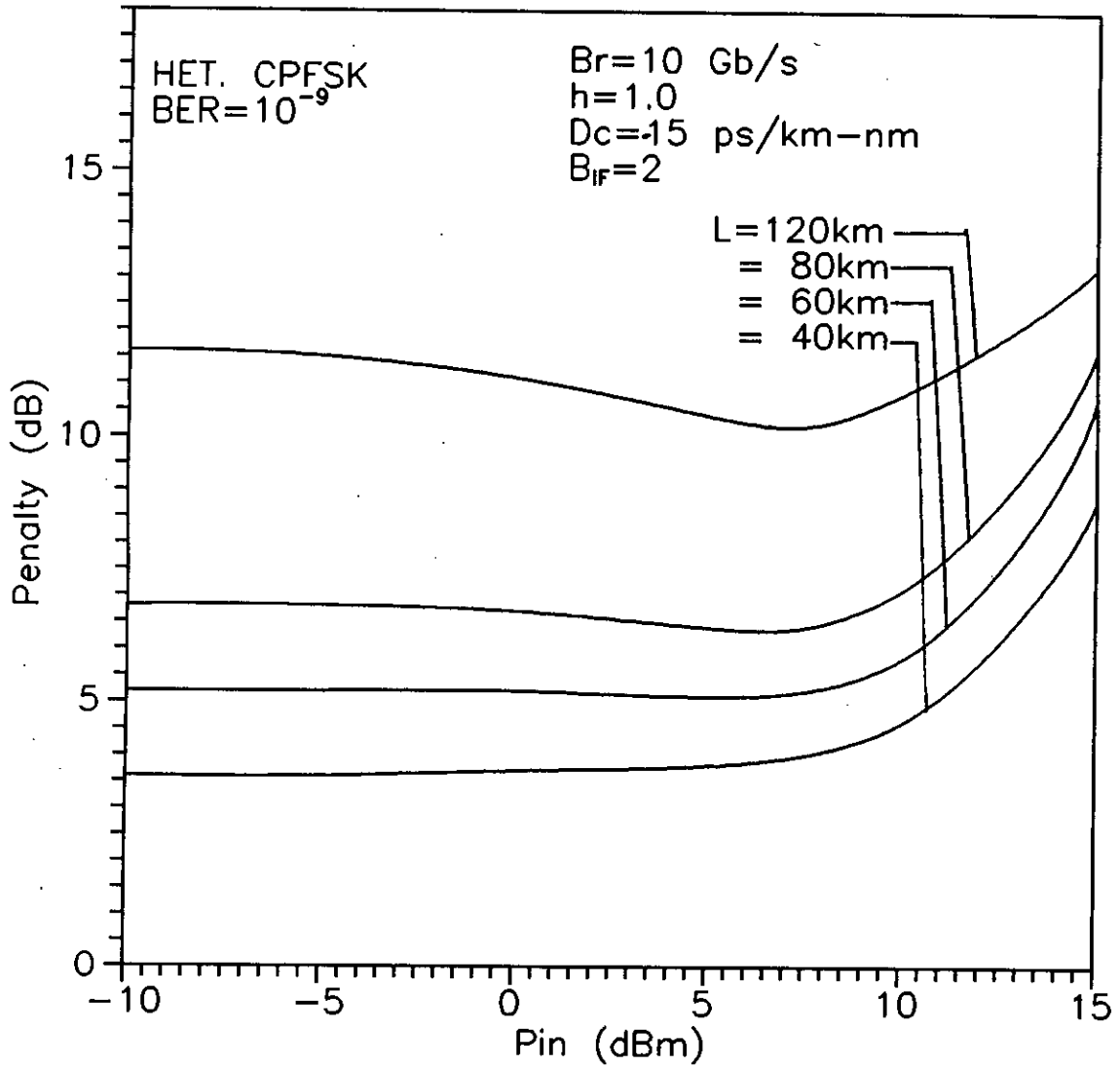


Fig.3.18 Plots of penalty in signal power due to Self-phase-modulation & fibre chromatic dispersion at BER= 10^{-9} versus power input with bit rate Br=10 Gb/s, dispersion co-efficient Dc=-15 ps/km-nm, band width B_{IF}=2 and modulation index h=1.0 for different lengths L=40km, 60km, 80km, 120km at a heterodyne CPFSK receiver.

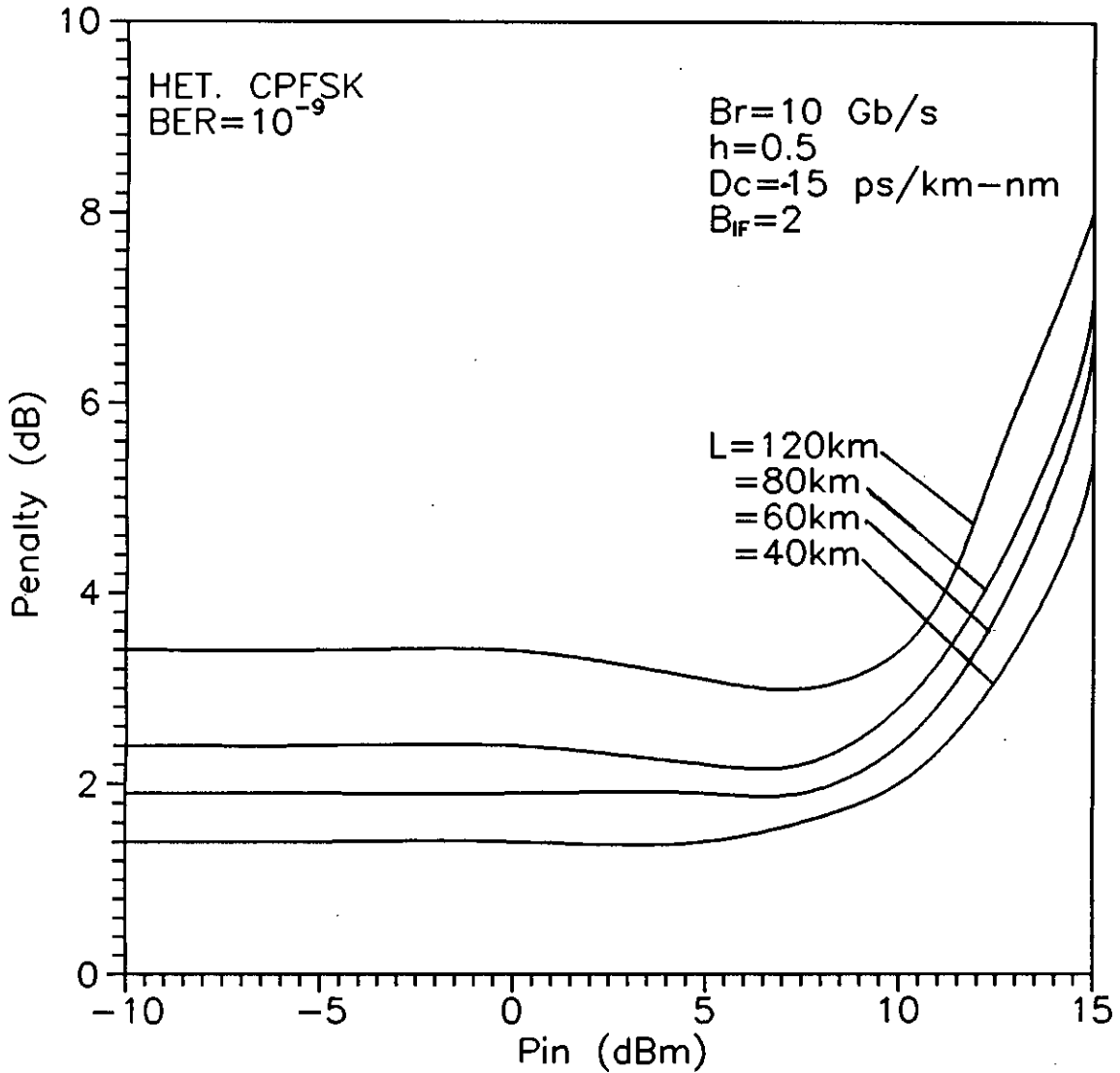


Fig.3.19 Plots of penalty in signal power due to Self-phase-modulation & fibre chromatic dispersion at BER= 10^{-9} versus power input with bit rate Br=10 Gb/s, dispersion co-efficient Dc=-15 ps/km-nm, band width B_{IF}=2 and modulation index h=0.5 for different lengths L=40km, 60km, 80km, 120km at a heterodyne CPFSK receiver.

penalty rises gradually where in direct detection CPFSK system it rises abruptly after 10.0 dBm and 12.5 dBm respectively. Penalty is higher for higher fibre length in all cases.

Similar plots of penalty versus input power are also shown in fig. 3.20 and fig. 3.21 for positive dispersion coefficient $D_c=15$ ps/km-nm at $h=1.0$ and $h=0.5$ respectively. Comparing to fig. 3.20 and fig. 3.21 it is found that penalty is less for $h=0.5$ than $h=1.0$ at positive dispersion coefficient. Again, it is observed that penalty remains constant up to a higher value of input power. For example, for $L=120$ km when $D_c=+15$ the penalty starts to increase after 0 dBm as in fig. 3.20, where as for $D_c=-15$, in fig. 3.18 penalty gradually decreases and starts to increase at or above 10 dBm.

For heterodyne CPFSK receiver, if the length L is increased from 40 km to 80 km the BER performance curve shifts to the right i.e. for same input power and received power BER is more, which is shown in fig. 3.22.

The variation of power penalty with modulation index h is plotted in fig. 3.23 and fig. 3.24 for heterodyne CPFSK receiver at fibre length $L=40$ km and 80 km respectively. It is observed that penalty increases almost linearly with increasing value of modulation index. For different values of input power three different curves have been plotted in same plot. When input power is 15 dBm penalty versus modulation index curve (fig. 3.23, 3.24) shows nonlinear characteristics. In this case penalty increases with higher slope up to $h=0.8$ and then degrades slowly.

A comparison of our analytical results is made in fig. 3.25 with the penalty measured from the eye-opening by simulation [40]. It is found that the analytical results are very close to those obtained by computer simulation and thus validates the approximations made in the analysis.

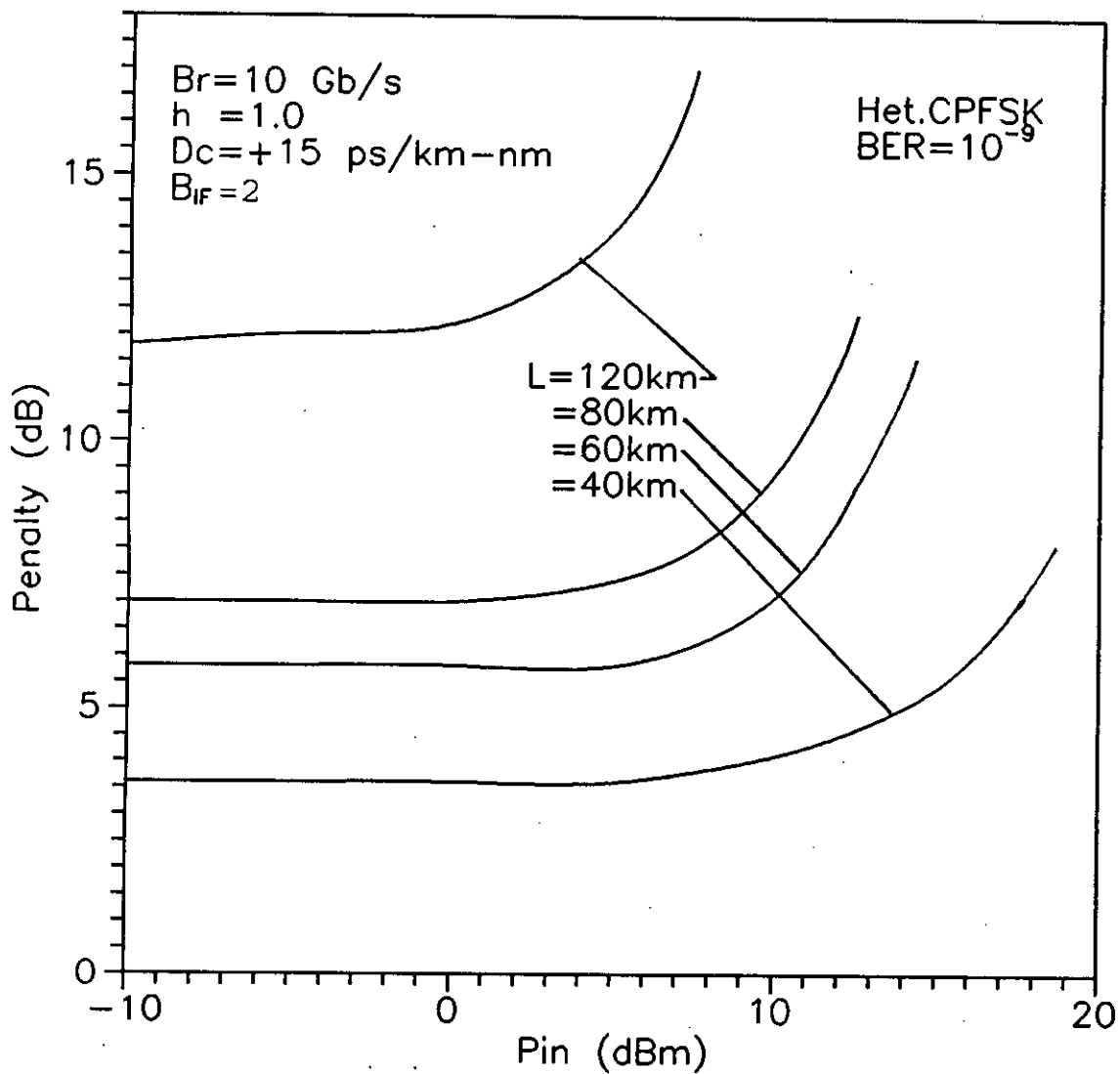


Fig.3.20 Plots of penalty in signal power due to Self-phase-modulation & fibre chromatic dispersion at $BER=10^{-9}$ versus power input with bit rate $B_r=10$ Gb/s, dispersion co-efficient $D_c=15$ ps/km-nm, band width $B_{IF}=2$ and modulation index $h=1.0$ for different lengths $L=40\text{km}$, 60km , 80km , 120km at a heterodyne CPFSK receiver.

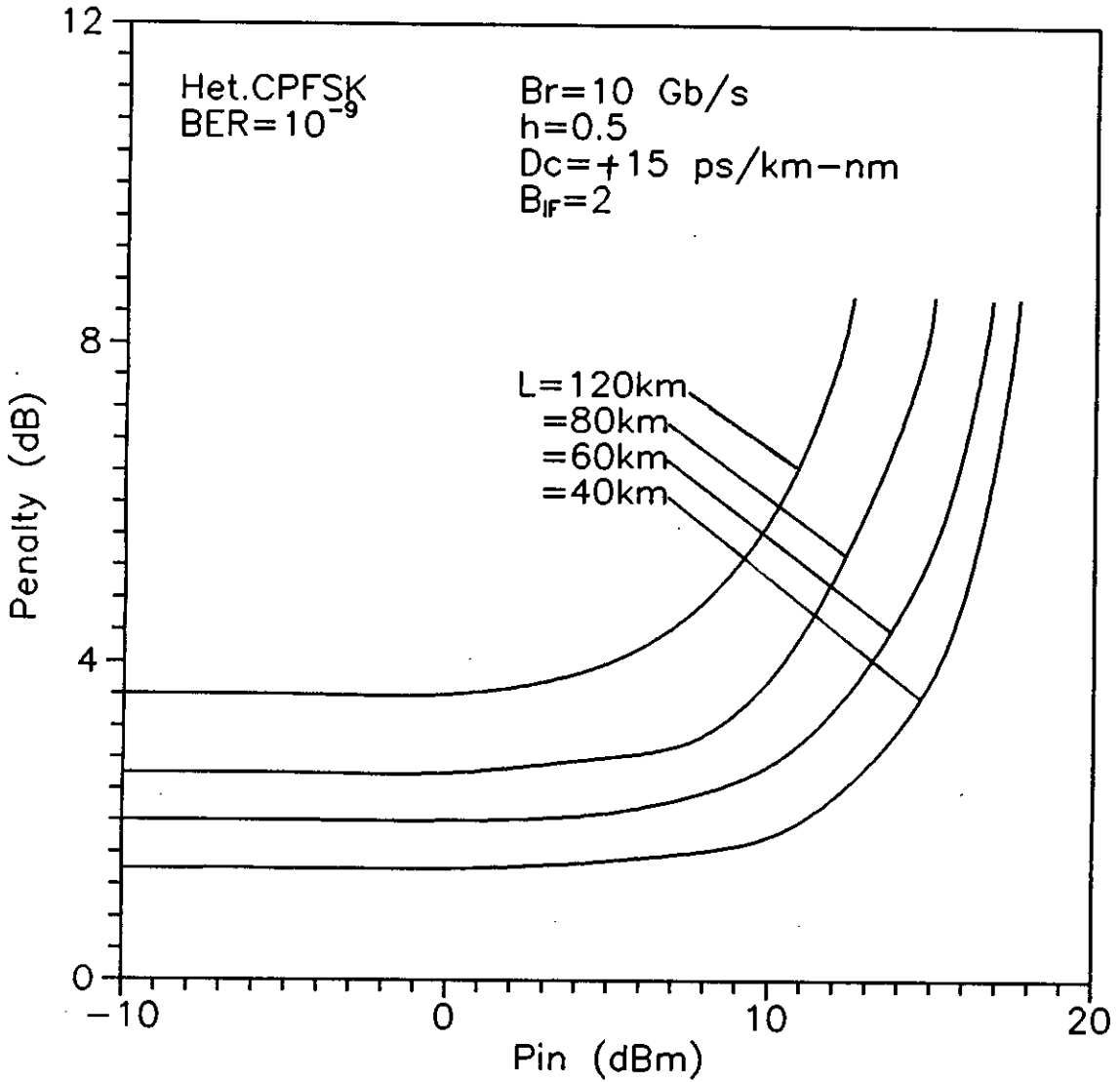


Fig.3.21 Plots of penalty in signal power due to Self-phase-modulation & fibre chromatic dispersion at BER= 10^{-9} versus power input with bit rate Br=10 Gb/s, dispersion co-efficient Dc=15 ps/km-nm, band width B_{IF}=2 and modulation index h=0.5 for different lengths L=40 km, 60 km, 80 km, 120km at a heterodyne CPFSK receiver.

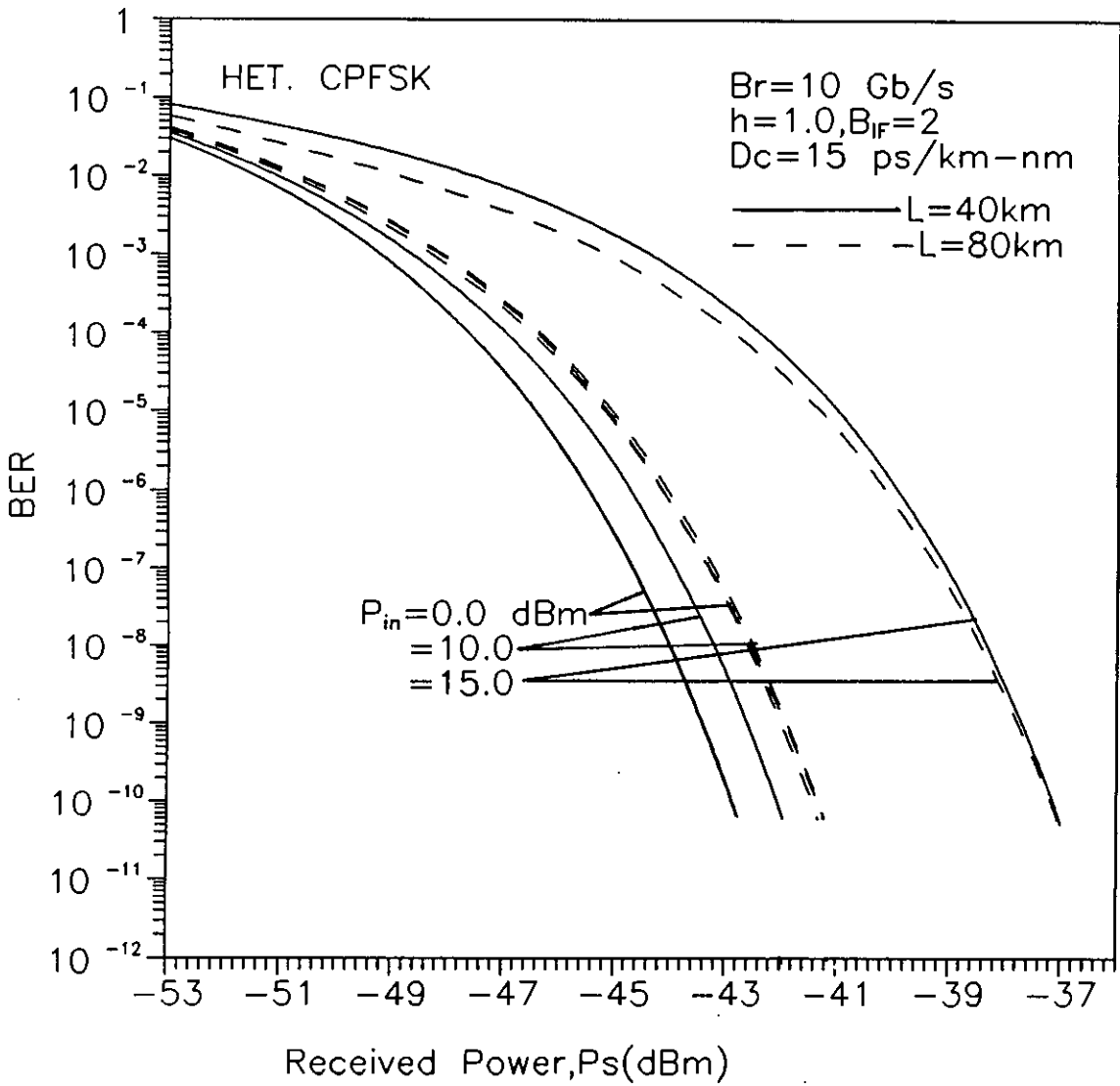


Fig3.22 Variation of the bit error rate (BER) performance due to different values of Length (say, $L=40,80\text{km}$) of a heterodyne CPFSK receiver at a bit rate 10 Gb/s with fibre chromatic dispersion $D_c=15 \text{ ps/km-nm}$, band width $B_{IF}=2$, for several values of received power P_s .

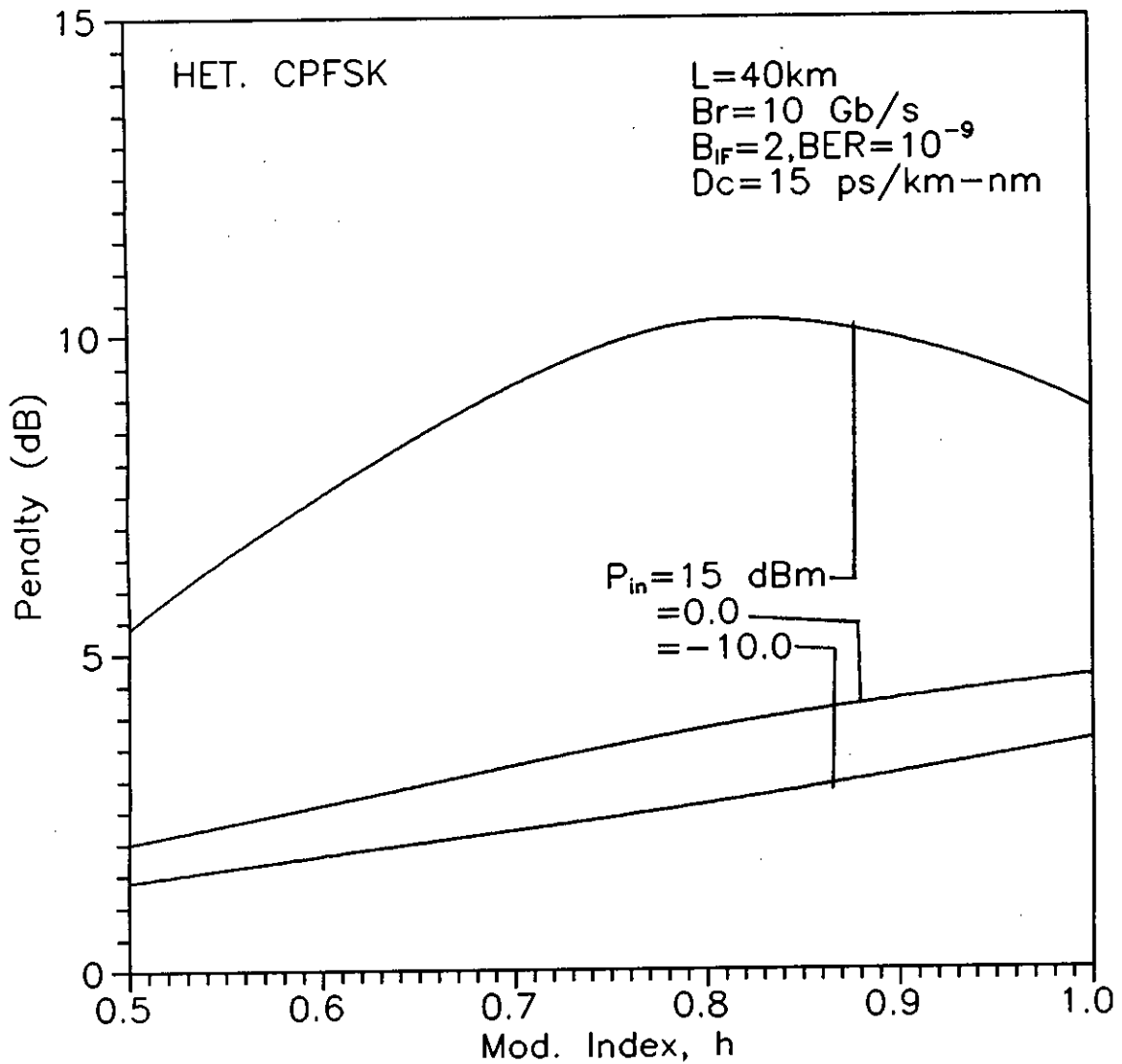
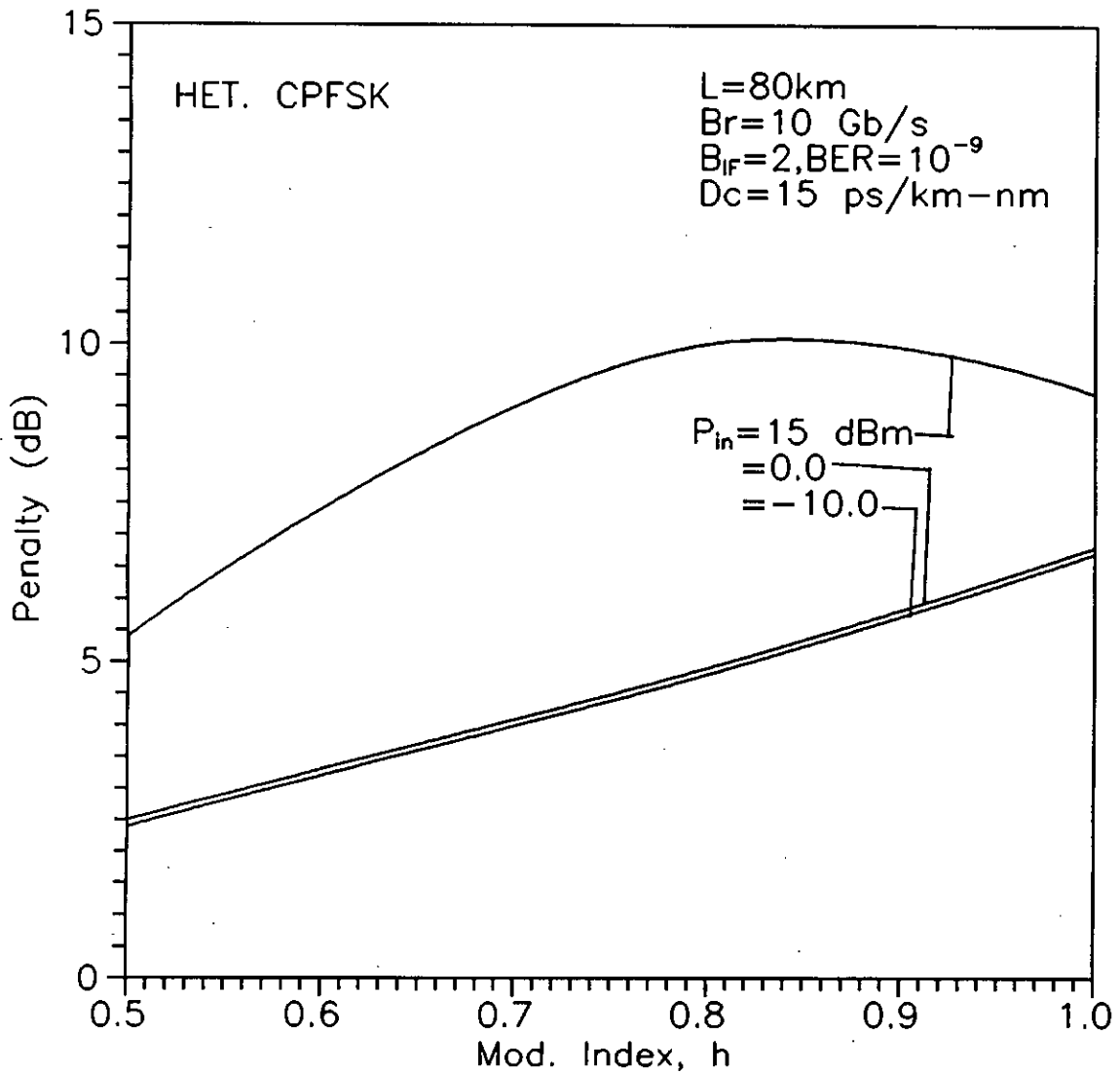


Fig.3.23 Variation of power penalty in signal power due to combined effect of Self-phase-modulation & fibre chromatic dispersion at $\text{BER}=10^{-9}$ versus modulation index (h) with fibre length $L=40\text{km}$, $B_r=10\text{ Gb/s}$, dispersion coefficient $D_c=15$ and band width $B_{IF}=2$ for different values of input power $P_{in}=-10, 0, 15\text{ dBm}$ for a heterodyne CPFSK receiver.



3.24

Fig.3.24 Variation of power penalty in signal power due to combined effect of Self-phase-modulation & fibre chromatic dispersion at $\text{BER}=10^{-9}$ versus modulation index (h) with fibre length $L=80\text{km}$, $B_r=10\text{ Gb/s}$, dispersion coefficient $D_c=15$ and band width $B_{IF}=2$ for different values of input power $P_{in}=-10, 0, 15\text{ dB}$ for a heterodyne CPFSK receiver.

92720

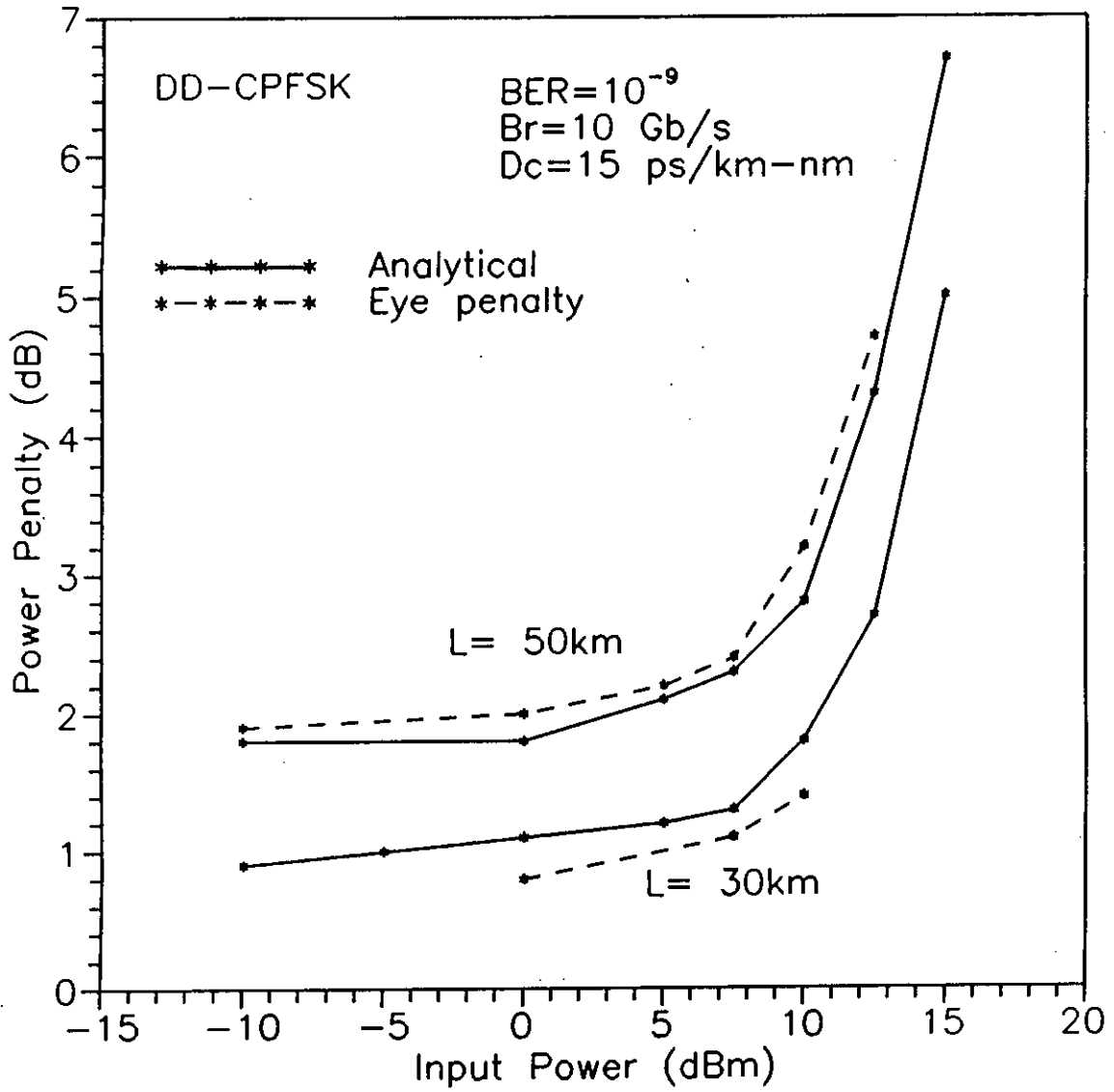


Fig.3.25 Comparison between analytical results with the penalty measured from eye-opening by simulation for fibre length $L=30 \text{ km}$ and 50 km at $BER=10^{-9}$, $Br=10 \text{ Gb/s}$, dispersion coefficient $Dc=15 \text{ ps/km-nm}$ and modulation index $h=1.0$ for direct detection CPFSK receiver.

Chapter-4

Conclusions and Suggestions for future works

4.1 Conclusions :

A theoretical analysis is provided for optical CPFSK transmission system with direct detection receiver and heterodyne CPFSK receiver using Mach-Zehnder Interferometer (MZI) as an optical frequency discriminator. The analysis is carried out to evaluate the combined effect of fibre chromatic dispersion and self phase modulation on the system performance. The probability density function (pdf) of the random phase fluctuation due to the effect of fibre chromatic dispersion and self phase modulation is determined from its moments and the expression for bit error probability is developed.

Following, the theoretical analysis the bit error rate performance results are evaluated at a bit rate of 10 Gb/s with single mode fibre at an wavelength of 1550 nm for different sets of values input power, modulation index, chromatic dispersion etc.

The results show that the performance of direct detection and heterodyne CPFSK system is highly degraded due to the effect of fibre dispersion and self phase modulation. For small values of dispersion coefficient D_c , the system suffers penalty in signal power at a specified BER of 10^{-9} compared to the case of no dispersion. In the presence of self phase modulation, the system performance is more degraded and the penalty is higher. For example, in presence of SPM the penalty suffered by the system at BER= 10^{-9} is approximately 2.2 dB for $D_c=15$, $P_{in}=5$ dBm, fibre span $L=80$ km and modulation index $h=1.0$, for direct detection receiver. It is further notice that the penalty is higher for higher values of modulation index. For example, when $L=40$ km, $D_c=15$, $P_{in}=5$ dBm; the penalty is

0.3 dB for $h=0.5$. Whereas the penalty is 1.0 dB for $h=1.0$. Similarly for heterodyne CPFSK receiver, penalty increases with increasing modulation index.

The power penalty increases with the increase of input power. The power penalty remains constant up to certain input power for a specified fibre length. But with the further increment of input power power penalty increases rapidly. For example, in direct detection CPFSK receiver up to input power $P_{in}=5$ dBm, $h=1.0$ and fibre length $L=40$ km, power penalty remains constant at 1.0 dBm but it starts to increase after 5 dBm and reaches to infinity after 15 dBm. Again it is observed that power penalty is comparatively lower for direct detection CPFSK receiver for $h=0.5$ but it shows infinite penalty quickly and sharply. For other cases with the variation of length penalty varies clearly i.e. for higher length higher penalty is observed.

Similarly for heterodyne CPFSK receiver, penalty versus input power curves shows similar variations. For higher distances rate of increment of penalty is higher. So we can conclude that penalty increases with increase in input power as well as length of fibre. The effect of SPM in presence of GVD thus imposes restrictions on the maximum allowable input power that can be launched into the fibre for a given fibre length and modulation index. For longer fibre span the effect of SPM is more and the allowable input power is highly restricted.

4.2 Suggestions for Future Works:

Further research related to this work can be carried out to investigate the influence of SPM on optical heterodyne FSK system with envelope detection receivers. The work can be extended to optical intensity modulation (IM) and differential phase shift keying (DPSK) transmission system with direct/ heterodyne detection receivers. Further investigations can also be initiated to analyze the performance of optical FSK/ DPSK systems with fibre having non-uniform chromatic dispersion along the fibre length.

Further works of importance are to determine dispersion compensation techniques to reduce the power penalty due to fibre chromatic dispersion so as to increase the repeaterless transmission distance in single/ multi channel transmission systems with single-mode fibres.

Further research related to this work can be carried out to investigate the influence of SPM on the performance of optical bi-direction ring network. The maximum number of channels, optimum channel separation, maximum fibre span limited by the combined effect of fibre chromatic dispersion and laser phase noise at a bit rate 10 Gb/s or higher are to be determine.

Further research works can also be carried out to evaluate the impact of fibre non-linear effect such as fibre Cross-phase-modulation (XPM) and Self-phase-modulation (SPM) on the performance of a WDM optical transmission systems.

REFERENCES :

- [1] J. R. Pierce, "Optical channel : practical limits with photon counting," IEEE Transaction on Communications, vol. com-26, no. 12, December 1978, pp. 1819-1821.
- [2] S. Kobayashi, Y. Yamamoto, M. Ito and T. Kimura, "Direct Frequency modulation in AlGaAs semiconductor lasers," IEEE Journal of Quantum Electron., vol. QE-18, no. 4, 1982, pp. 582-595.
- [3] K. Iwashita and T. Matsumoto, "Modulation and detection characteristics of optical continuous phase FSK transmission system," Journal of Lightwave Technology, vol. LT-5, April 1987, pp. 452-260.
- [4] R. S. Vodhanel, J. L. Gimlett, N. K. Cheung and S. Tsuji, "FSK heterodyne transmission experiments at 560 Mbit/s and 1 Gbit/s," Journal of Lightwave Technology, vol. LT-5, April 1987, pp. 461-468.
- [5] K. Nosu, H. Toba and K. Iwashita, "Optical FDM transmission technique," Journal of Lightwave Technology, vol. LT-5, no. 9, 1987, pp. 1301-1308.
- [6] R. S. Vodhanel, A. F. Elrefaie, M. Z. Iqbal, R. E. Wagner, J. L. Gimlett and S. Tsuji, "Performance of directly modulated DFB lasers in 10 Gb/s ASK, FSK and DPSK Lightwave systems," Journal of Lightwave Technology, vol. 8, no. 9, September 1990, pp. 1379-1385.

- [7] N. Takato, T. Kominato, A. Sugita, K. Jinguji, H. Toba and M. Kawachi, "Silica based integrated optic Mach-Zehnder multi/demultiplexer with channel spacing of 0.01-250 nm", IEEE Journal on Selected Areas in Communication, vol.8, no.6, August 1990, pp. 1120-1127.
- [8] C. Rolland, R. S. Moore, F. Shepherd and G. Hillier, "10 Gb/s, 1.56 μm multi quantum well InP /InGaAsP Mach-Zender optical modulator," Electronic Letters, vol. 29, no. 5, March 1993, pp. 471-472.
- [9] H. Toba, K. Oda, K. Nosu, N. Takato and H. Miyazawa, "5 GHz spaced eight channel optical FDM transmission experiment using guided wave tunable demultiplexer," Electronic Letters, vol. 24, 1988, pp. 78-80.
- [10] A. R. Chraplyvy, "Limitations on Lightwave communications imposed by optical fiber nonlinearities," Journal of Lightwave Technology, vol. 8, no. 10, October 1990, pp. 1548-1557.
- [11] A.R. Chraplyvy, "Limitation of lightwave communication imposed by optical-fibre nonlinearities", J. Lightwave Technology, vol. 8, no. 10, March 1991, pp. 1548-1557.
- [12] D. Cotter, "Stimulated Brillouin scattering in mono mode optical fiber," J. Opt. Communications, vol. 4, 1983, pp. 10-19.
- [13] "Effect of fibre nonlinearity on long distance transmission", J. Lightwave Tech. vol. 9, no. 1, pp. 121-128, Jan. 1991.

- [14] Robert G. Waarts, A. A. Friesem, "Nonlinear Effects in Coherent Multi-channel Transmission Through Optical Fibres" Proceedings of the IEEE, Vol. 78, No. 8, August 1996, pp. 1344-1367.
- [15] K. O. Hill, D. C. Johnson, B. S. Kawasaki and I. R. MacDonald, "CW three-wave mixing in single mode optical fibers," J. Appl. Phys., vol. 49, 1978, pp. 5098-5106.
- [16] J.P. Hamaide, Ph. Emplit and J.M. Gabriagues, "Limitation in long haul IM/DD optical fibre systems caused by chromatic dispersion and nonlinear kerr effect", Electron Lett., vol. 26, no. 18, pp. 1451-1453.
- [17] I. Garrett and G. Jacobsen, "Phase noise in weakly coherent systems," IEE proceedings- J. opto electronics, vol. 136, 1989, pp. 2179-2180.
- [18] A. F. Elrefaie and R. E. Wagner, "Chromatic dispersion limitations for FSK and DPSK systems with direct detection receivers," IEEE Photonics Technology Letters, vol. 8, no. 1, January 1991.
- [19] I. Garrett, "Introduction to the effect of phase noise on coherent optical system," Proceedings of Forth Tirrenia International workshop on digital communication, Tirrenia, Italy, September 19-23, 1989, pp. 103-116.

- [20] D. J. Malyon and W. A. Stallard, "565 Mb/s FSK direct detection system operating with four cascaded photonic amplifiers," *Electronics Letters*, vol. 25, no. 8, 1989, pp. 495-496.
- [21] B. L. Patel, E. M. Kimber, M. G. Taylor, A. N. Robinson, I. Hardcastle, A. Hadjifotiou, S. J. Wilson, R. Keys and J. E. Righton, "High performance 10 Gb/s optical transmission system using Erbium-doped fiber amplifier," *Electronic Letters*, vol. 27, no. 23, November 1991, pp. 2179-2180.
- [22] D. Marcuse, "Single-channel operation in very long nonlinear fibres with optical amplifiers at zero dispersion", *J. Lightwave Tech.* vol.8, no.10, pp.1548-1557, Oct. 1990.
- [23] M.J.O'Mahony, "Progress in optical amplifiers", *Proceedings of the Fourth Tirrenia International Workshop on Digital Communications*, Tirrenia, Italy, Sep.19-23, 1989, pp.73-84.
- [24] N.A. Olsson, "Lightwave systems with Optical Amplifiers", *Journal of Lightwave Technology*, vol.7, pp. 1071-1082, July 1989.
- [25] N.Antoniades, I.Roudas, R.E.Wagner, and S.F.Habiby, "Simulation of ASE noise accumulation in a wavelength add/drop Multiplexer Cascaded" *IEEE Photonics Technol. Lett.*, vol.9, Sep. 1997.
- [26] D.J. Malyon, T.Widdowson, E.G.Bryant, S.F.Carter, J.V. Wright and W.A. Stallard, "Demonstration of optical pulse propagation over 10000 km of fibre using recirculating loop", *Electron Lett.*, vol. 27, no. 2, pp. 120-121, 1991.

- [27] G.E. Wickens, D.M. Spirit and L.C. Blank, "Nonlinear transmission of 20 Gbit/s optical time-division-multiplexed data, over 205 km of dispersion shifted fibre", *Electron. Letter.* vol.28, no.2, pp. 117-118,1992.
- [28] B. Glance, K. Pollock, C. A. Burrus, B. L. Kasper, G. Eisenstein and L. W. Stulz, "Density spaced WDM coherent optical star network," *Electronic Letters*, vol. 23, 1987, pp. 875-876.
- [29] M.J. Potasek, G.P. Agrawal and S.C. Pinault, "Analytic and numeric study of pulse broadning in nonlinear dispersive optical fibres", *J. Opt. Soc. Am. B*, vol.3, no.2, pp. 205-211, 1986.
- [30] G.P. Agrawal, *Nonlinear Fibre Optics*. New York: Academic, 1989.
- [31] M. Stern, J.P. Heritage, R.N. Thurston, and S. Tu, "Self-Phase Modulation and dispersion in high data rate fiber-optic transmission system", *J. Lightwave Technology*, vol. 8, no. 7, July 1990. pp. 1009-1015.
- [32] Nobuhiko Kuchi and Shinya Sasaki, "Analytical Evaluation Technique of Self-Phase-Modulation Effect on the Performance of Cascaded Optical Amplifier Systems", *J. Light wave Tech.* vol. 13, no-5, May 1995.
- [33] Md. Abdul Moqaddem, "Performance Analysis of Direct Detection Optical FSK in the Presence of Fibre Chromatic Dispersion", M.Sc. Engineering thesis submitted to the Dept. of Electrical & Electronic Engineering, BUET, June,1996.

- [34] Mohammad Jahangir Alam, "Performance Study of Optical Coherent and Direct Detection DPSK Systems in Presence of Fibre Chromatic Dispersion", M.Sc. Engineering thesis submitted to the Dept. of Electrical & Electronic Engineering, BUET, August,1996.
- [35] E.Bedrosin and S.O.Rice, "Distorsion and crosstalk of linearly filtered, angle-modulated signals," Proc.IEEE, vol.56, pp.2-13, 1968.
- [36] E.Forestieri and G.Prati, "Theoretical Analysis of Coherent Optical FSK Systems with Limitter-Discriminator Detection," IEEE Trans. Commun.,vol.42. pp.562-573, 1994.
- [37] R. Gangopadhya, S.P. Majumder, P. Cochrane and E. Forestieri, "Performance Analysis of a Direct Detection Receiver for AMI coded CPFSK Signals", IEEE Photon. Technol. Lett.,vol.7, pp.552-554, May1995.
- [38] PRABHU, V.K.; Some considerations of error bounds in digital systems', Bell Syst. Tech. Journal,1971,50,pp. 3127-3150.
- [39] S.P.Majumder. R.Gangopadhyay, E.Forestieri and G.Prati, "Sensitivity penalty for AMI-coded CPFSK in heterodyne delay demodulation receiver," IEEE Photon. Technol. Lett., vol.7, pp.1207-1209, 1995.

[40] S.P.Majumder, R.Gangopadhyay and B.Pal "Sensitivity Penalty for Direct Detection CPFSK receiver due to Laser phase Noise and Chromatic Dispersion", submitted to IEEE Photon. Tech. Letter, 1997.

[41] S.Benedetto, E.Biglieri, and V.castellani, "Digital Transmission Theory", (Prentice Hall Inc., New Jersey, 1987).

